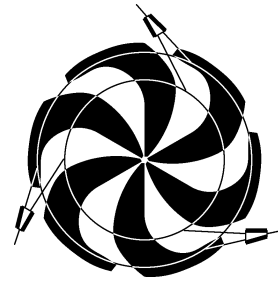


# TRIUMF



## ANNUAL REPORT SCIENTIFIC ACTIVITIES 2001

ISSN 1492-417X

**CANADA'S NATIONAL LABORATORY  
FOR PARTICLE AND NUCLEAR PHYSICS**

OPERATED AS A JOINT VENTURE

MEMBERS:

THE UNIVERSITY OF ALBERTA  
THE UNIVERSITY OF BRITISH COLUMBIA  
CARLETON UNIVERSITY  
SIMON FRASER UNIVERSITY  
THE UNIVERSITY OF VICTORIA

ASSOCIATE MEMBERS:

THE UNIVERSITY OF MANITOBA  
McMASTER UNIVERSITY  
L'UNIVERSITÉ DE MONTRÉAL  
QUEEN'S UNIVERSITY  
THE UNIVERSITY OF REGINA  
THE UNIVERSITY OF TORONTO

UNDER A CONTRIBUTION FROM THE  
NATIONAL RESEARCH COUNCIL OF CANADA

OCTOBER 2002

*The contributions on individual experiments in this report are outlines intended to demonstrate the extent of scientific activity at TRIUMF during the past year. The outlines are not publications and often contain preliminary results not intended, or not yet ready, for publication. Material from these reports should not be reproduced or quoted without permission from the authors.*

# ISAC PROJECT

## INTRODUCTION

This has been the first full year of ISAC-I operation. Accelerated radioactive ion beams were successfully transported to both the TUDA and DRAGON stations allowing the nuclear astrophysics experimental program to commence. The year has also been a beneficial learning experience for operations and maintenance personnel, experimenters, accelerator personnel and beam schedulers. The initial investment in engineering has paid off. The proton beam on target has been gradually increased as maintenance experience was gained and now 20 kW driver beam powers are operational. Long target lifetimes are being observed. Target exchanges and module repairs can be accomplished with very little personnel exposure. Contamination has been successfully contained as planned. A second target station had been envisioned to reduce the servicing impact on beam scheduling. In response to user demand for more beam time, a major initiative this year has been the fabrication of the east target station. The second target station will increase the number of scheduled hours each year, provide a quick backup for early target failures, reduce the risk when developing new targets, and provide additional isotopes by accommodating an ECR ion source. New target materials, beams and ion sources are being developed.

ISAC-II is rapidly becoming a reality. Immediately following provincial government funding approval for ISAC-II civil construction, an aggressive schedule was adopted. A team was put into place that transformed a concept based on requirements into a cost-effective facility design. By year-end the design was nearly ready to be sent out for tender. Significant progress also occurred on the technical front. The collaboration with ISN (Grenoble) has successfully characterized an ECR charge state booster to a point where a purchasing decision could be made and many components of the ECR have now been ordered. Beam dynamics studies of the linac have refined the superconducting accelerator layout. A prototype superconducting cavity was built in collaboration with INFN-LNL (Legnaro) and successfully tested. A cryostat has been built at TRIUMF and characterization of the cavity will continue in a newly refurbished laboratory.

## ISAC OPERATIONS

This year was the first complete year of operation of the ISAC-I low energy facility. The first quarter was devoted to shutdown activities. Beam schedule 99 began in the second quarter and carried on through the summer and, in parallel, the accelerator team com-

missioned the high energy systems using beam from the off-line ion source (OLIS). Beam schedule 100 began in the fourth quarter and continued until year-end. There was less reliance on beam physicists during routine beam operation of LEBT although their assistance was always welcomed. The MEBT and HEBT beam operation required extensive support from the beam dynamics experts. A typical change of energy through the accelerators required three or more hours of procedures – including documenting the existing parameters, switching to a stable pilot beam, adjustment of the energy and retuning of matching elements, documentation, then switching to RIB. Most operators have been able to proceed on their own after a few assisted energy changes, but there are still occasions that challenge even the experts. The members of the ISAC Operations group take great pride in their contributions to the successes of the experiments and major ISAC milestones that have been highlighted elsewhere in this Annual Report.

Operational performance statistics are provided for the ISAC beam production of RIB from ITW and stable beam from OLIS. These are summarized separately for each beam schedule in Tables XVII–XXVIII. In some instances OLIS was used by an on-line experiment as part of procedures to change mass or energy. Other times it was used for commissioning or when the RIB was unavailable, such as during a maintenance period. As a single user facility of RIB, there is an incentive to minimize activation when the beam is not required. This is done by stopping the RIB on a Faraday cup in the target station and, for longer periods, turning off the proton beam. For Operations purposes, these appear as “off” time for each experiment. Some of this time may be due to a cool down period during an acquisition cycle, or overhead for the experiment such as changing of samples or collection tapes. Therefore care must be taken in using these statistics for analyzing the efficiency of the scheduled experiment beam time usage. The off time is included in the hours recorded as available for RIB. For most systems, the downtime is a sum of many various problems, e.g. for controls, related to the programmable logic controller hardware and EPICS program. “Beam line 2A unavailable” indicates times when the proton beam is off for a variety of reasons including scheduled cyclotron maintenance. “ISAC idle” includes time when the proton beam may have been available but, in the absence of system failures, ISAC RIB was not delivered, e.g. when trained operators were not available or experiments were unable to take beam, etc. In schedule 99, the major faults were the failure of a

target high current connector which resulted in a HV problem; a thermal relay problem in IMS:MB1; and a failure of the OLIS waveguide Y-bend. In schedule 100, the major problems were related to the weather – high winds causing a lengthy site power outage, and heavy rains resulting in perimeter drains backing up into the building, eventually causing water damage on LEBT HV feedthrough. Over the year, RIB was available for 2,390.2 hours out of 3505 hours scheduled, for a combined cyclotron/ISAC system performance of 68.2%.

Training for the accelerated beam operation was provided by way of 22 formal lectures, and by informal on-the-job training by the beam dynamics experts during operation. As with the LEBT systems, the lectures were videotaped for future use in the training of new operators. Setting up of a systematic approach to training (SAT) program and completion of an ISAC Operations Manual have been high priority tasks falling into the capable hands of Mike Hauser, the training and documentation coordinator. These activities are

complementary to each other and progress on one is helpful to the other. The Documentation Manual was given a higher priority and was very near to completion at year-end. Development of the training program will resume in 2002. Another development was the implementation of a Web-based work permit system. This was provided by coop student Wendy Wiggins under the supervision of Chris Payne.

In the control room, a new console desk was installed. It has permitted the addition of a second layer of monitors to display the many controls and graphics that are required for the operators to be effective in beam delivery. It will also permit more operations in parallel, which has been a severe limitation and source of frustration in these early days. In the coming year, in addition to providing beam for the scheduled experiments and performing systems maintenance, the major effort will be to establish and complete the SAT training program for ISAC operators.

Table XVII. ISAC beam schedule 99: April 25 – September 5 (weeks 17–36). ITW beam to ISAC experiments (hours).

Experiment number	Scheduled	Actual	Tune	Off
$\beta$ -NMR commissioning	264.00	10.75	13.70	65.15
E815 ( $\beta$ -NMR)	312.00	237.25	7.85	15.10
E823 (GPS2)	300.00	149.05	16.05	3.65
E826/828 (LTNO)	192.00	43.45	40.40	60.35
E863 (LTNO)	156.00	89.25	22.45	0.00
Yield	120.00	57.15	26.30	2.40
Mass separator development	48.00	12.00	0.00	0.00
E812 (TOJA)	336.00	159.25	29.90	98.90
Total	1,728.00	758.15	156.65	245.55

RIB available  $758.15 + 156.65 + 245.55 = 1,160.35$  hours.

Combined cyclotron/ISAC performance  $1,160.35/1,728.00 = 67.1\%$ .

Table XVIII. ISAC beam schedule 99: April 25 – September 5 (weeks 17–36). Breakdown of ITW radioactive beams to ISAC experiments (hours).

Isotope	$\beta$ -NMR comm.	E815 $\beta$ -NMR	E823 GPS2	E826/828 LTNO	E863 LTNO	Yield	Mass separator development	E812 TOJA	Total
$^7\text{Li}^*$	7.75	4.75				1.00		12.50	26.00
$^8\text{Li}$	3.00	232.50				0.20		140.00	375.70
$^{16}\text{O}^*$								+6.75	6.75
$^{23}\text{Na}$						0.75			0.75
$^{39}\text{K}$						13.60	12.00		25.60
$^{74}\text{Rb}$			118.75			0.25			119.00
$^{75}\text{Ga}$					88.05	0.50			88.55
$^{75}\text{Rb}$						0.50			0.50
$^{79}\text{Rb}$				0.65					0.65
$^{80}\text{Rb}$			30.30		0.90				31.20
$^{84}\text{Rb}$					0.30				0.30
$^{85}\text{Rb}^*$				6.50					6.50
$^{91}\text{Rb}$				36.30					36.30
Other						40.35			40.35
Total	10.75	237.25	149.05	43.45	89.25	57.15	12.00	159.25	758.15

\* stable beam

+ from OLIS

Table XIX. ISAC beam schedule 99: April 25 – September 5 (weeks 17–36). ITW systems downtime and overhead.

ISAC system	Hours
Controls	15.65
Magnet power supplies	9.70
MEBT rf	0.50
OOPS	2.00
Polarizer	2.25
RFQ	1.35
Site power	2.00
Target station (HV breakdown)	182.30
OTHER	
Beam line 2A unavailable	148.10
Cyclotron maintenance	181.35
Cyclotron development/training	23.90
ISAC idle	41.25
ISAC startup	4.60
ISAC cooldown	92.00
Target changes	73.50
Target/ion source conditioning	46.00
Procedures	19.40
ITW/LEBT tuning	121.15
HEBT tuning	8.65
Shutdown	48.00
Total	1,023.65

Table XX. OLIS operation June 4 – September 5 (weeks 23–36). Beam to ISAC experiments (hours).

Experiment number	Scheduled	Actual	Tune	Off
DRAGON commissioning	468.00	159.80	45.15	180.80
E812 (TOJA)	360.00	126.40	52.90	182.60
E879 (TUDA)	360.00	159.60	16.30	98.60
Test (LTNO)	0.00	1.25	8.00	5.00
Total	1,188.00	447.05	122.35	467.00

Beam available  $447.05 + 122.35 + 467.00 = 1,036.40$  hours  
 OLIS performance  $1,036.40/1,188.00 = 87.2\%$

Table XXI. OLIS operation June 4 – September 5 (weeks 23–36). Breakdown of OLIS beams to ISAC experiments (hours).

Isotope	DRAGON commissioning	E812 TOJA	E879 TUDA	Test LTNO	Total
<sup>12</sup> C				0.50	0.50
<sup>13</sup> C		119.65			119.65
<sup>14</sup> N				0.75	0.75
<sup>15</sup> N	65.90				65.90
<sup>16</sup> O	93.90	6.75			100.65
<sup>21</sup> Ne			159.60		159.60
Total	159.80	126.40	159.60	1.25	447.05

Table XXII. OLIS operation June 4 – September 5 (weeks 23–36). OLIS systems downtime and overhead.

ISAC system	Hours
Controls	5.75
DTL rf	24.40
HEBT rf	2.15
Charge-exchange stripper	3.50
MEBT rf	1.45
Pre-buncher	1.00
RF controls	5.50
RFQ	6.00
Safety	1.40
Site power	1.50
Ion source	44.75
OTHER	
ISAC maintenance	330.90
Development	2.20
ISAC idle/no user	531.60
ISAC startup	2.00
Procedures	171.10
MEBT tuning	0.40
HEBT tuning	12.00
Total	1,147.60

Table XXIII. ISAC beam schedule 100: September 26 – December 3 (weeks 39–51). ITW beam to ISAC experiments (hours).

Experiment number	Scheduled	Actual	Tune	Off
E815 ( $\beta$ -NMR)	372.00	265.40	3.10	26.60
E824 (DRAGON)	660.00	382.10	30.65	18.70
E879 (TUDA)	541.00	396.40	12.80	3.85
E903 (Osaka)	48.00	57.20	0.00	0.00
Yield	84.00	32.05	1.00	0.00
Mass separator development	72.00	0.00	0.00	0.00
<b>Total</b>	<b>1,777.00</b>	<b>1,133.15</b>	<b>47.55</b>	<b>49.15</b>

RIB available  $1,133.15 + 47.55 + 49.15 = 1,229.85$  hours

Combined cyclotron/ISAC performance  $1,229.85/1,777.00 = 69.2\%$

Table XXIV. ISAC beam schedule 100: September 26 – December 3 (weeks 39–51). Breakdown of ITW radioactive beams to ISAC experiments (hours).

Isotope	E815 $\beta$ -NMR	E824 DRAGON	E879 TUDA	E903 Osaka	Yield	Total
$^7\text{Li}^*$	30.75					30.75
$^8\text{Li}$	234.65			3.00		237.65
$^9\text{Li}$				54.20		54.20
$^{21}\text{Na}$		382.10	396.40		0.55	779.05
Other					31.50	31.50
<b>Total</b>	<b>265.40</b>	<b>382.10</b>	<b>396.40</b>	<b>57.20</b>	<b>32.05</b>	<b>1,133.15</b>

\* stable beam

Table XXV. ISAC beam schedule 100: September 26 – December 3 (weeks 39–51). ITW systems downtime and overhead.

ISAC system	Hours	ISAC system	Hours
		OTHER	
Controls	17.90	Heavy rainfall	8.00
DTL rf	1.45	Beam line 2A unavailable	146.70
Electrostatic power supplies	2.35	Cyclotron & ISAC maintenance	170.70
Magnet power supplies	7.90	Cyclotron development/training	70.45
MEBT rf	2.15	ISAC idle	25.30
OOPS	2.55	ISAC startup	12.00
Polarizer	6.15	Target changes	38.50
RF controls	0.50	Shutdown	72.00
RFQ	1.90	Target/ion source conditioning	65.75
Safety	0.25	Procedures	129.50
Services	5.00	ITW/LEBT tuning	83.55
Site power	38.65	RFQ tuning	0.75
Target station	34.75	MEBT tuning	0.30
Vacuum	7.95	DTL tuning	0.70
	cont'd.	HEBT tuning	1.50
	<b>Total</b>		<b>955.15</b>

Table XXVI. ISAC beam schedule 100: September 26 – December 3 (weeks 37–51). OLIS beam to ISAC experiments (hours).

Experiment number	Scheduled	Actual	Tune	Off
DRAGON commissioning	216.00	112.70	13.55	6.30
E824 (DRAGON)	204.00	157.35	20.60	37.85
E879 (TUDA)	48.00	*81.30	7.80	1.50
8 $\pi$ commissioning	0.00	3.50	0.00	0.00
Total	468.0	354.85	41.95	45.65

\*was to have received ITW beam ( $^{21}\text{Na}$ ), but ITW was not ready

Beam available  $354.85 + 41.95 + 45.65 = 442.45$  hours

OLIS performance  $442.45/468.00 = 94.5\%$

Table XXVII. ISAC beam schedule 100: September 26 – December 3 (weeks 37–51). Breakdown of OLIS beams to ISAC experiments (hours).

Isotope	DRAGON commissioning	E824 DRAGON	E879 TUDA	8 $\pi$ commissioning	Total
$^{14}\text{N}$				3.50	3.50
$^{21}\text{Ne}$	112.70	157.35	81.30		351.35
Total	112.70	157.35	81.30	3.50	354.85

Table XXVIII. ISAC beam schedule 100: September 26 – December 3 (weeks 37–51). OLIS systems downtime and overhead.

ISAC system	Hours
Controls	8.70
Diagnostics	0.25
DTL rf	11.65
Electrostatic power supplies	0.60
HEBT rf	3.35
Magnet power supplies	8.70
MEBT rf	3.00
Charge-exchange stripper	0.40
RF controls	2.00
RFQ	1.00
Site power	42.50
Ion source	93.30
Vacuum	0.65
OTHER	
ISAC maintenance	363.75
Development	4.20
ISAC idle/no user	1,238.30
Startup	12.50
Shutdown	108.00
Procedures	133.15
OLIS/LEBT tuning	11.70
RFQ tuning	3.30
MEBT tuning	4.20
DTL tuning	4.90
HEBT tuning	18.45
Total	2,078.55

The history of operation of ISAC production targets is given in Table XXIX. Several target changes were performed this year. Schedule 99 started with a target of niobium foils. Shortly after startup, it began to spark and consequently operation was compromised, resulting in delivery of beam at a reduced energy. On inspection at a rescheduled early target change, it was discovered that a high current connection had failed due to a design flaw, and the insulators on the target service tray were coated with vaporized metal. The tray was exchanged remotely in the south hot cell. These activities are discussed in the remote handling report. The service took about 7 weeks, beam off to beam on. The next target was one of tantalum foils and was in operation for a total of 17,279  $\mu\text{A h}$  at a proton current of about 20  $\mu\text{A}$ . Finally, a target of SiC pellets was used for delivery of Li beams to the high energy area. It received 16,010  $\mu\text{A h}$  with most operation at beam currents up to 15  $\mu\text{A}$ . Until the east target station is commissioned, the turn around for a target change is about ten days. This includes a two day cool down period, five days to effect the change and three days for conditioning of the new target.



Table XXIX. ISAC target history.

Target ID	In date	Out date	Charge $\mu\text{A h}$	Thickness $\text{g}/\text{cm}^2$	Power $\mu\text{A h} \times$ $\text{g}/\text{cm}^2$	Comments
CaO #1	25-Nov-98	15-Dec-98	70	36.00	2,520.0	Failure due to EE short
CaO #2	20-Dec-98	15-May-99	363	31.10	11,289.3	Failure due to EE short
Nb foils #1	14-Jul-99	20-Oct-99	3,242	11.10	35,986.2	Failure due to TBHT-t/c problem
Nb foils #2: R1	01-Nov-99	09-Dec-99	3,149	11.50	36,213.5	Removed for 100 $\mu\text{A}$ tests
Dump only	10-Dec-99	10-Dec-99	43	0.00	0.0	100 $\mu\text{A}$ test
Talbert	17-Dec-99	12-Jan-00	197	10.00	1,970.0	100 $\mu\text{A}$ test
Nb foils #2: R2	17-Mar-00	04-Jun-00	5,913.8	11.50	68,008.7	Total: Nb foils #2 R1 + R2
Ta foils #1	10-Jun-00	19-Jul-00	3,515.83	21.25	74,711.4	Removed for $\text{CaZrO}_3$
$\text{CaZrO}_3$ #1 R1	24-Jul-00	21-Aug-00	518.7	42.27	21,925.4	9.45 g $\text{Ca}/\text{cm}^2$ , 21.51 g $\text{Zr}/\text{cm}^2$
$\text{CaZrO}_3$ #1 R2	02-Oct-00	18-Nov-00	838.0	42.27	35,422.3	9.45 g $\text{Ca}/\text{cm}^2$ , 21.51 g $\text{Zr}/\text{cm}^2$
SiC #1 R1	18-Nov-00	10-Apr-01	2,155.0	7.43	16,011.6	7.43 g $\text{SiC}/\text{cm}^2$ : 5.05 g $\text{Si}/\text{cm}^2$ , 2.38 g $\text{C}/\text{cm}^2$
Nb foils #3:R1	13-Apr-01	31-May-01	3,766.0	22.00	82,852.0	1026 foils – 40 $\mu\text{A}$ rating
Ta foils #2	08-Jul-01	13-Sep-01	17,279.0	43.60	753,364.4	1026 foils – 40 $\mu\text{A}$ rating
SiC #2 R1	18-Sep-01	16-Jan-02	16,010.0	29.90	478,699.0	29.9 g $\text{SiC}/\text{cm}^2$

## SAFETY AND RADIATION CONTROL

### Licensing

An application to construct the ISAC-II facility was prepared and sent to the Canadian Nuclear Safety Commission (CNSC) late in 2001. The application was accompanied by a safety analysis report that described the hazards associated with the proposed operation of ISAC-II and the design features that will mitigate these hazards. It is expected that the licence will be issued early in 2002.

### Access Control and Radiation Monitoring

The ion beam radiation monitoring system (IBRMS) was expanded to accommodate the operation of the ion beam accelerator system and the high-energy experiments as well as a number of changes to the layout of the low energy beam lines. A users manual was also published for this system. The target storage facility in the target maintenance hall was included in the target hall access control interlock system so as to allow access only when the target storage facility shielding door is closed. Design was started on incorporating the interlocks for the east target station. Considerable effort went into standardizing the interlock requirements for high-voltage systems. All new systems will be expected to conform to these standards and some systems may need to be retrofitted.

### Commissioning

Radiation surveys were performed during the commissioning of the DTL section of the ISAC accelerator system. The primary source of radiation is the X-rays generated by the parasitic acceleration of electrons. RF

power levels were established that limit the X-ray production to acceptable levels during access to the DTL shielding enclosure. The access control system for the accelerator enclosure will be interlocked so that access is allowed only when the rf power is below these levels.

## REMOTE HANDLING GROUP

### Target Modules

Following design revisions for the second generation ISAC east target station modules, work began on assembly of new target, exit, entrance and dump modules by Remote Handling personnel. Although these modules are similar to the west station in design, changes to the containment box and services duct require new assembly procedures.

### Target Hall

The target hall is being prepared for a more demanding, two-station, higher current beam schedule by the end of 2002. Provision for improved safety and contamination control included additional cleaning and radiation sampling stations set up within the hall, and an intermediate monitor check established adjacent to the target station access area. Contamination control blanket tarpaulins have been provided throughout the hall, and lock-up safety procedures have been reviewed to better suit routine hall work activities.

The largest new target hall project for the year was the shielded spent targets storage vault that was designed, assembled and commissioned in the spring. This unit is remotely accessible by the target hall crane and allows interim storage of up to twenty-four individual spent targets and two larger bins for component trays, all for later re-use or eventual disposal.

## Hot Cell Facility/Targets

Installation of the access shielding doors, and double chain drive modifications to the turntable have now completed the major hot cell construction. Refinement of operations has included new tooling for connecting gas-line equipped targets, and the fitting of a breathable air system into the hot cell service anteroom.

A catastrophic failure in target module #1 required the full month of June for hot cell repair. Poor electrical conduction of a target oven heater connection, inside the lower containment box, vaporized material plating many of the high voltage insulators. This required entire replacement of the target/extraction column assembly to be performed remotely. The containment box was opened, additional holes drilled/tapped, all services disconnected, the extraction column support tray removed, a new assembly installed and services re-connected and tested by manipulator operation. This was a first-time hot cell endeavour for this magnitude of work.

Commissioning of the target hall spent target storage vault was completed and four previously irradiated targets (CaZrO<sub>3</sub> #1, SiC #1, Nb #3, Ta #2), as well as the damaged TM #1 extraction column, are now stored in the vault for future re-use or disposal.

During the year there were three remote target changes performed on target module #1 (Nb #3, Ta #2, SiC #2). The Ta #2 target heat shield was removed in the hot cell to examine physical characteristics of the high power (40  $\mu$ A) run. The target oven tube was found to be distorted by heat expansion and the method of mounting.

Two surface source extraction columns were assembled this year; the replacement for the damaged TM #1 column, and one intended for the conditioning box. Assembly of a third extraction column for TM #2 has begun.

Design of a test apparatus for decontaminating materials has been completed and assembly is under way. Design work began on a manipulator support/installation cart for easier replacement and servicing of the hot cell master-slave manipulators.

## Remote Crane System

The control console for the remote crane was improved with additional closed circuit video monitors, switching and console racks. A laser ranging system was installed on the crane down-hall travel motion, providing more accurate feedback for remote crane operations.

## ISAC TARGETS AND BEAMS

In 2001 the ISAC operating licence was upgraded to allow unlimited 100  $\mu$ A  $p^+$  beam current operation

for all target materials with the exception of actinide targets. Two targets (Nb #3 and Ta #2) have now operated with proton currents up to 40  $\mu$ A. This is calculated to be the limit of the target design originally intended for beam currents in the range of 1–3  $\mu$ A. Additionally, a ceramic pellet target (SiC #2) was operated for an extended period with a proton current of 15  $\mu$ A to deliver <sup>21</sup>Na beams to the ISAC accelerators and the TUDA and DRAGON experimental stations.

At the beginning of the 2001 ISAC run schedule, the Nb #3 foil target was installed to provide <sup>74</sup>Rb beams for Expt. 823, and <sup>79</sup>Rb beams for Expt. 828/LTNO. The Nb #3 target consisted of 1026 Nb foils (0.025 mm thickness) with a total target thickness of 22 g Nb/cm<sup>2</sup>. The target thickness, volume and foil surface area were approximately double that of the previous Nb foil targets. Throughout the Nb #3 target running period, there were problems with breakdowns of the target high voltage system. The inability of the target module to maintain a 30 kV beam energy precluded <sup>8</sup>Li beam delivery to the polarizer and  $\beta$ -NMR experimental station. In spite of the voltage problems, the target run lasted from April 17 to May 24. The Nb #3 target received 3766  $\mu$ A h of beam and was operated at proton currents up to 40  $\mu$ A. Yields of Li, Rb and Ga radionuclides were measured as a function of proton current.

At the end of the Nb #3 running period, inspection of the target revealed that a steel washer had overheated and evaporated metal onto the high voltage insulators. The target support structure and extraction electrode system were removed from the target module and replaced with a new unit. Removal and replacement operations were performed inside the ISAC hot cell using remote handling techniques. The replacement procedure was successfully completed during June and the target module was ready for installation of a new target in early July.

The Ta #2 target consisted of 1050 Ta foils (0.025 mm thickness) with a total target thickness of 43.6 g Ta/cm<sup>2</sup>. As with the Nb #3 target, the Ta #2 target had approximately twice the total thickness, volume and foil surface area of the previous Ta #1 target. The yields of Li isotopes were measured as a function of proton current up to a maximum of 40  $\mu$ A. A <sup>11</sup>Li ( $t_{1/2} = 8.5$  ms) yield of  $2.2 \times 10^4$ /s was achieved at 40  $\mu$ A. Ta #2 operated from July 16 to September 5 and received a total of 17,279  $\mu$ A h of proton beam, the equivalent of  $3.9 \times 10^{20}$  protons. For most of the running period, it operated with a 20  $\mu$ A proton beam delivering <sup>8</sup>Li beams of  $2 \times 10^8$ /s to the ISAC accelerators. The <sup>8</sup>Li was the first accelerated radioactive beam at ISAC. Ta #2 currently holds the record for being the longest operational ISAC target.

To date, the second longest-lived ISAC target is SiC #2. This target was in operation from October 3 to December 18 supplying accelerated  $^{21}\text{Na}$  beams to Expts. 824 and 879 at the DRAGON and TUDA experimental stations, polarized  $^8\text{Li}$  to Expt. 815 at the  $\beta$ -NMR station and the first polarized  $^9\text{Li}$  beam for initial calibrations for Expt. 903 and the polarimeter station. The SiC #2 target consisted of 163 pressed pellets of SiC + 10% molar excess graphite powder. The average pellet thickness was 1.2 mm with an average pellet density of  $1.73\text{ g/cm}^3$ . The  $29.9\text{ g SiC/cm}^2$  thickness was approximately 4 times the thickness of the previous SiC #1 target. Initial target operation started on October 3 with a proton current of  $3\text{ }\mu\text{A}$  for Expt. 879, followed by  $15\text{ }\mu\text{A}$  operation in November for the other experiments. The initial  $^{21}\text{Na}$  yield at  $15\text{ }\mu\text{A}$  was  $2.5 \times 10^9/\text{s}$  while that of  $^{22}\text{Na}$  was  $2 \times 10^{11}/\text{s}$ . Both yields were observed to slowly decrease with time, finishing with  $5 \times 10^8/\text{s}$  and  $5 \times 10^{10}/\text{s}$ , respectively, towards the end of the run on December 6. Total proton beam charge was  $16,010\text{ }\mu\text{A h}$ , corresponding to  $3.6 \times 10^{20}$  protons on target.

## ION SOURCES FOR ISAC

### Electron Cyclotron Resonance (ECR) Source

The design of a radiation hard ECR source for the ISAC radioactive beam facility has been completed.

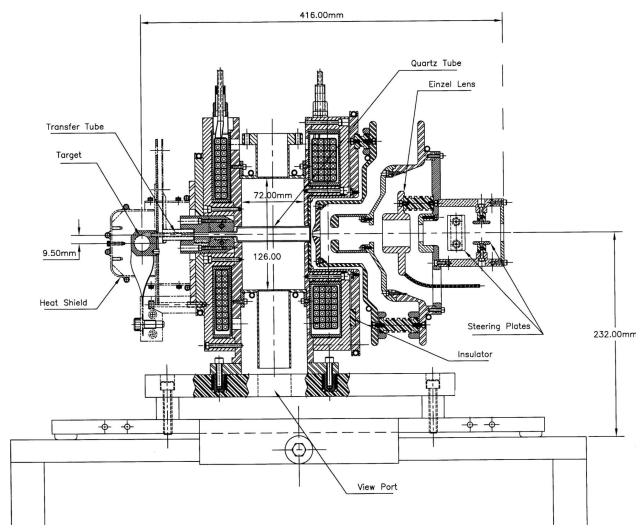


Fig. 141. The radioactive isotopes produced at the target drift toward a quartz tube located inside the cavity of a 2.45 GHz electron cyclotron resonance (ECR) ion source. A unique feature of this source is that the quartz plasma chamber is considerably smaller ( $\sim 80$  times) than the resonant cavity in order to increase the efficiency for the extraction of short half-life isotopes. This ion source has a high efficiency for ionizing gaseous species in a single charge state. This source will be used to produce ion beams of nitrogen, oxygen, and neon from zeolite targets, as well as that of Xe, Kr, Ar, and Cl isotopes using Ta, Nb, and CaO targets, respectively.

The ion source with its 0–60 kV extraction system is coupled to the radioactive isotope production target via a small transfer tube (Fig. 141). For a typical ISAC target, the copper coils of the ECR source will be exposed to a dose rate of about  $10^5\text{ Gy/h}$  for a  $100\text{ }\mu\text{A}$  – 500 MeV incident proton beam. The whole assembly will be located beneath a 2 m thick steel shielding structure.

The fabrication of the source is nearing completion. It will be tested in the ion source test stand (ISTS) during the first half of 2002. A new vacuum chamber has been built to accommodate the ECR source in the ISTS. Figure 142 shows the source under assembly. This source will be installed in the east target module during the second half of 2002.

### Off-Line Ion Source (OLIS)

The source operated satisfactorily throughout 2001 delivering more than 5200 hrs of a variety of beams. It continued to provide helium, nitrogen and neon beams to the RFQ, DTL, MEBT, and HEBT for accelerator studies. It also supplied  $^{21}\text{Ne}$ ,  $^{15}\text{N}$ ,  $^{24}\text{Mg}$ , and  $^{13}\text{C}$  beams for the DRAGON and TUDA experiments. Although the microwave source, installed at the OLIS terminal, was designed to produce beams only from gaseous elements, it could also supply the Mg beam, however, at a cost: damage due to sputtering shortens the lifetime of the source. For the low energy area, OLIS delivered  $^{14}\text{N}^{2+}$  beam to tune the Osaka and  $\beta$ -NMR beam lines.

Since beams of alkaline and metallic elements are being requested by several experimental groups on a regular basis, a new concept for the off-line ion source was proposed. The new OLIS terminal will house three sources: the present microwave source for gaseous

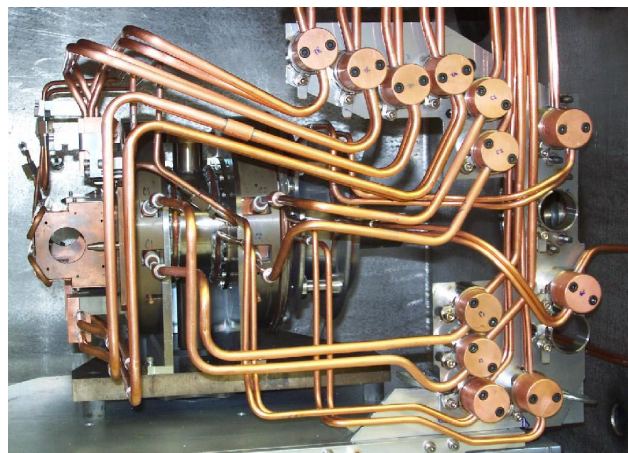


Fig. 142. The target ion source extraction assembly on a self-aligning tray. This picture shows the combined current, voltage and cooling quick disconnect feeder lines. The target-ion source is serviceable via remote handling.

beams, a surface ion source for alkaline beams, and a source to produce metallic beams. In spring, 2002 the new terminal with initially two sources will be assembled. The installation of the source for metallic beams is foreseen in 2003. The future OLIS terminal will be capable of producing almost all ions requested by the experimental groups.

### Charge State Booster (CSB)

The research collaboration program set up between the Institut des Sciences Nucleaires (ISN-Grenoble) and TRIUMF to study the properties of the ISN-PHOENIX-ECR source as a charge breeder device was brought to completion in November, 2001. The result of these measurements indicates that this system can fulfill TRIUMF requirements in terms of breeding efficiency and breeding time of the  $1^+/n^+$  process. A sample of some gaseous, metallic and alkaline elements relevant to the ISAC experimental programs (such as Ar, In, Ag, Zn, Sn, Sr, Ga, Co, Rb, K and Na) was studied. The results are listed in Table XXX. Based on these results, an order will be placed in January, 2002 to acquire the PHOENIX source from PANTECHNIK (France). This firm has been licensed by ISN to manufacture the source based on the ISN design.

This source will be incorporated as an extension to the TRIUMF  $1^+$  ion source test stand in 2002–03 for further tests and in preparation for its future installation in the ISAC-I hall.

Table XXX. The breeding efficiency,  $\eta$ , and time,  $\tau$ , for various isotopes.

	$\eta(\%)$	$\tau(\text{ms})$
$^{40}\text{Ar}^{1+}/6^+$	5	100
$^{115}\text{In}^{1+}/18^+$	4.6	120
$^{109}\text{Ag}^{1+}/17^+$	3	75
$^{64}\text{Zn}^{1+}/10^+$	2.8	50
$^{120}\text{Sn}^{1+}/19^+$	4.1	150
$^{88}\text{Sr}^{1+}/14^+$	3.6	125
$^{69}\text{Ga}^{1+}/11^+$	2	80
$^{59}\text{Co}^{1+}/9^+$	2	100
$^{85}\text{Rb}^{1+}/13^+$	5	100
$^{39}\text{K}^{1+}/9^+$	7.9	70
$^{23}\text{Na}^{1+}/8^+$	1.8	–

### ISAC POLARIZER

At the beginning of the year, the following laser system changes were made to increase the  $^8\text{Li}$  polarization:

a) The mode spacing of the Ti:sapphire dual-frequency laser was accurately measured by observing the beat frequency between the two modes, and was corrected to precisely match the 382 MHz  $^8\text{Li}$  ground state hyperfine splitting.

b) The laser frequency was locked to a frequency-stabilized He-Ne laser, thus reducing laser drift to approximately 3 MHz/hour. This obviated the previous need to vary the Na cell bias to compensate for laser drift.

c) Acoustically-generated noise on the laser frequency was reduced from approximately 40 to 20 MHz RMS by placing a vibration damping layer between the water-cooled argon-ion pump laser and the laser table. Water cooling to the Ti:sapphire laser remains the largest contributor to frequency noise.

d) Smaller apertures were placed on the Na vapour target (reduced to 12 mm from 16 mm) and the He gas target (reduced to 8 mm from 10 mm), to maximize overlap between the ion and laser beams. The smaller apertures reduced the overall transmission efficiency by a factor of 0.82.

e) A 19 MHz electro-optic phase modulator (EOM) was ordered to artificially increase the instantaneous laser frequency bandwidth of  $\sim 1$  MHz. Such an EOM placed in the laser beam produces cw laser frequency sidebands at 19 MHz intervals. The purpose was to ensure that  $^8\text{Li}$  atoms are always near resonance with the laser or the sidebands during their  $2 \mu\text{s}$  transit time in the polarizer. Without the sidebands, many atoms would not see the laser due to the acoustically-generated noise on the laser frequency. It was also thought that the likely Doppler-broadened absorption width of the beam was  $\sim 40$  MHz.

The first polarized  $^8\text{Li}$  run, scheduled for May, was almost completely lost due to target ion source problems. However, very important information was obtained over three shifts about the energy spread in the beam. Laser induced fluorescence from a 20 keV  $^7\text{Li}$  beam showed that multiple collisions in the Na vapour created a low energy tail in the beam that could be eliminated by reducing the Na vapour density (unfortunately reducing the neutralization yield at the same time). The energy width at typical Na densities was approximately 5 eV or, equivalently, over 100 MHz absorption bandwidth in a 30 keV  $^8\text{Li}$  beam. The energy spread in the incident beam was less than 2 eV (FWHM).

In light of the above knowledge, as well as polarization calculations that showed it was advantageous to optically pump at more closely spaced frequency intervals, another 28 MHz EOM was obtained in time for the next polarized  $^8\text{Li}$  run in August. Combining the two EOMs in series easily permitted broadening of the laser to cover 100 MHz, as well as providing finely spaced frequencies at about 10 MHz intervals. That was a big success, and transverse  $^8\text{Li}$  polarizations of up to 70%, saturated with laser power, were measured at the polarimeter. (The original longitudinal polariza-

tion is converted into transverse polarization by a  $90^\circ$  electrostatic bend just before the polarimeter. The polarimeter is described in the LEBT section.) However, calculations showed that the polarization under our experimental conditions should have been nearly 100%. The apparent loss of polarization will require further investigation. The August run marked the commissioning of the ISAC polarizer as an experimental facility.

The final run in November/December was used to continue the  $\beta$ -NMR data-taking begun in August, and to polarize  $^9\text{Li}$  for the first time at ISAC. Experiment 903 requires highly polarized  $^{11}\text{Li}$ , but sufficient beam was not available using the SiC ISAC target. The more easily produced isotope,  $^9\text{Li}$ , was used to check neutron detectors and other apparatus. Since the ground state hyperfine splitting is different in  $^8\text{Li}$  and  $^9\text{Li}$ , only one of the dual laser frequencies could be used for optical pumping. Both ground state levels were optically pumped, however, using a tunable EOM to create laser sidebands 852 MHz either side of the main laser frequencies, thus matching the  $^9\text{Li}$  hyperfine splitting. The combination of the dual-frequency laser and EOM reduced the effective laser power by a factor of one-third, which may explain the low polarization that was achieved. The polarization was thought to be 30–40%, although the latest information on  $^9\text{Li}$   $\beta$ -decay branching ratios implies that the polarization was half that. The final run was also used to test Cs vapour as the neutralizer target. It was hoped that its smaller excitation energy than Na and greater mass would produce less energy broadening in the beam. Not unexpectedly, the neutralization yield was lower, since Cs also yields  $\text{Li}^-$  ions, but unfortunately the energy broadening was also worse than with Na.

In future, a high power, single frequency ring laser and EOM combination must be used to achieve high polarization of any isotope other than  $^8\text{Li}$ . Our experience with the old Spectra-Physics ring laser mentioned in last year's report has been disappointing. It is no longer supported by the manufacturer, which has in fact abandoned the field, and despite a significant effort, it is still not functioning properly. At year-end, the decision was made to buy a new ring dye laser from Coherent Inc. in time for the next polarized run.

## BEAM DYNAMICS

### Theory

Canonical transformations have been found which eliminate the derivatives of strength functions in dipole benders. Previously, this has been achieved for quadrupoles. This allows simple calculation of lowest-order aberrations without any detailed knowledge of fringe field shapes.

### Software

The beam transport code TRANSOPTR has been ported to Linux. Aberration calculations have been added for both magnetic and electrostatic dipole benders. As well, a Wien filter has been added.

A general electrostatic bender has been written for COSY- $\infty$ .

### Hardware Designed

The new 3-way bender design has been used to re-design OLIS (off-line ion source). This will allow 3 different sources to be attached, to broaden the selection of stable ions.

A new section of beam line has been designed and built, and commissioning has started. This is for the  $8\pi$  experiment. It is located in place of GPS1, which has in turn been relocated to the ILE section.

Additional commissioning of the  $\beta$ -NMR platform has been done. In this post-polarizer section of beam line, two additional branches have been designed and installed: a polarimeter, and a beam line section for the Osaka experiment.

### ISAC CONTROLS

Detailed design and implementation of additional sections for the ISAC control system proceeded smoothly and the following major milestones were achieved:

- Vacuum, optics and diagnostics control for the HEBT beam line beyond the Prague magnet.
- Vacuum, optics and diagnostics control for the TUDA and DRAGON beam lines as well as the TUDA experiment.
- Upgrades to the laser control and stabilization for the ILE2 beam polarizer.
- Vacuum, optics and diagnostics control for the ILE2A1 polarimeter.
- Vacuum control for the Osaka (ILE2A3) beam line.
- Vacuum, optics and diagnostics control for the  $8\pi$  experiment (ILE1A) beam line.

During the year, control for approximately 500 new devices was added to the ISAC control system, bringing the total to 1850 controlled devices.

### Hardware

Two new VME crates were added to the control system, one to separate the control of the ILE1 and ILE2 beam lines and a second to back up the overloaded HEBT IOC.

An additional PLC breakout cabinet was built, pre-wired, and installed for the vacuum systems of the DRAGON beam line. All vacuum devices for the

HEBT, HEBT2, and HEBT3 beam lines, as well as for the DRAGON experiment, were connected and commissioned. The vacuum controls for the  $8\pi$  beam line and the Osaka experiment beam line were commissioned.

160 new CAN-bus controllers were installed for the supplies of the HEBT and TUDA, DRAGON and  $8\pi$  beam lines.

Development was started on a separate EPICS control system for a target conditioning station, consisting of a vacuum box with ion source, and a beam line with analyzing magnet. A PLC breakout panel was installed and hook up to the vacuum devices is complete.

The control system wiring documentation was made available on the Controls group's Web server. For easy access, screen dumps of the EPICS synoptic screens are incorporated in HTML pages. The Web buttons, which in the control system call up device control panels, call up the wiring diagrams for the respective devices. For semi-automatic maintenance of this documentation, an auto-print program was written to generate PDF files from the documentation drawings. Perl scripts connect these PDF files automatically to the Web page buttons.

## Software

The PLC ladder logic programs for the vacuum systems of HEBT, TUDA, DRAGON,  $8\pi$  and Osaka beam lines were tested and commissioned.

ISAC standard EPICS display pages and supporting scripts were created for all new subsystems. Device control panels for all new optics and diagnostics devices were created using the edd display editor.

This year saw a continuation of efforts to enhance the ISAC relational device database (IRDB) and automate the production of new controls subsystems.

The process for automatic generation of vacuum device control panels was refined and the first generation of panels was put into production. These panels improve the interlock visualization and contain hyperlinks to control panels for devices, which are involved in interlocks [Keitel, ICALEPCS 2001, San Jose, November 27–30 (in press)].

The automatic generation of CAPFAST subsystem schematics based on reports from the IRDB is now the standard process for generating EPICS runtime databases. Missing information from subsystems, which had been installed during the previous years, was added to the IRDB. Now all subsystem schematics are generated and updated automatically [Keitel and Nussbaumer, *ibid.*]. Force and bypass summary screen generation was reworked, to achieve a consistent look and feel with other panels.

Laser control of the ILE2 beam polarizer [Nussbaumer *et al.*, *ibid.*] had performance and reliability of

the closed loop stabilization system improved. The system is now capable of maintaining laser stabilization for periods of many hours without operator intervention. A control strategy has been developed using custom software, and will be the basis for planned future performance upgrades. Areas for additional reliability upgrades have been identified.

Control support was added for the MEBT bunch rotator, MEBT chopper, and HEBT buncher rf systems, as well as for the new OLIS beam attenuators.

For the Prague magnet and the MEBT dipole magnets, closed-loop current stabilization was implemented based on feedback from the hall probes.

Beam line scaling algorithms were developed for DRAGON and for the accelerator physicists.

For the target commissioning station, the PLC program and all EPICS software for the vacuum system controls were developed and commissioned; work on the optics and diagnostics systems is in progress.

## System and Development Support

Two more SUN workstations were added in order to remove some software development bottlenecks. A considerable amount of time had to be spent on system maintenance for the development and production machines in order to catch up on operating system upgrades, rationalizing of configurations, and enhancing security.

A Linux-based firewall was installed, which separates the ISAC control system IOCS, PLCs, SUN application servers and Linux consoles from the rest of the TRIUMF site.

More documentation, tutorial material and troubleshooting information was added to the ISAC controls Web site.

During the mini-shutdown in September, the EPICS software was upgraded to the latest stable release 3.13.5 without any significant problems.

An attempt was also made to upgrade the IOC operating system to vxWorks release 5.4, in order to make use of the Tornado II tools. This upgrade led to networking and performance problems, which could not be resolved in the time available. The upgrade was rolled back to vxWorks 5.3 without problems.

Toward the end of the year, preparations for the installation of the second ISAC target station were under way. The conceptual design calls for independent operation of the east and west stations. This will require the installation of two more PLCs and significant modifications to the existing ladder software.

## Commissioning and Operation

During this year, we saw a transition from commissioning of large subsystems to commissioning of



smaller systems in parallel with regular beam delivery. The simultaneous operation of radioactive and stable beams was successfully supported. This mode, however, made it increasingly difficult to schedule enough time for enhancements, reliability improvements and regular maintenance. The conversion of the operations console PCs from Windows to Linux was completed and resulted in considerably reduced frustration levels of the operations crew. During the shutdown periods, Chris Payne from ISAC operations was again a valuable addition to the Controls group.

## RF SYSTEMS

### RFQ

The RFQ operated reliably for the various settings of this year's beam commissioning and production. The only troubles experienced for a few weeks in spring were the spontaneous trips caused by ac power ripples or transients. The problem was tackled with filtering and delaying signals in the amplifier interlock circuits. High power pulsing has been performed once to reduce the buildup of dark currents.

### MEBT

#### Bunch rotator

The triple gap split ring 106 MHz buncher devoted to bunch rotation in the MEBT was commissioned this year and operated very reliably. The tank, originally fabricated for the prototype DTL buncher, was modified to accept a new bunch rotator structure. Development and fabrication were done at INR RAS, Russia. Tuning and tests were accomplished at TRIUMF. The buncher is specified for rather moderate effective voltage of 80 kV and consumes about 5 kW at full power. This device at start up requires an rf conditioning for up to half an hour. The bunch rotator at assembly phase is shown in Fig. 143.

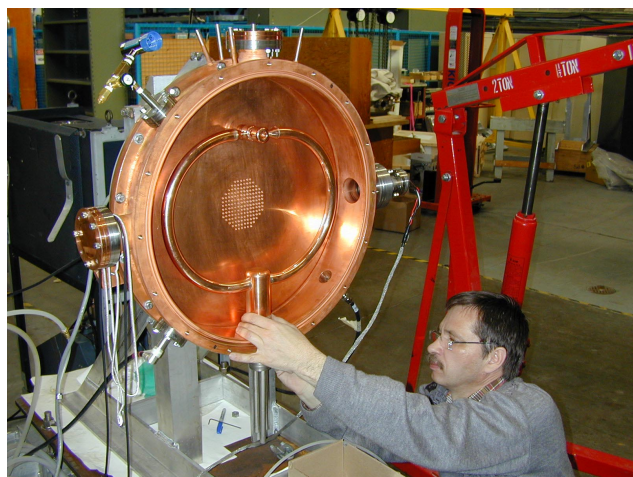


Fig. 143. Bunch rotator assembly.

### Choppers

The dual frequency chopper was commissioned this year and operated very reliably. Structurally, it consists of two independent rf systems of 5.9 MHz and 11.8 MHz but is combined in a common housing box. In addition to rf voltage, a dc bias is applied to the chopper plates. The chopper requires relatively low voltages, maximum of about 7 kV, and didn't show any problem in operation. Figure 144 shows the dual frequency chopper with open covers. The bunch rotator and chopper installed in the MEBT line are shown in Fig. 145.

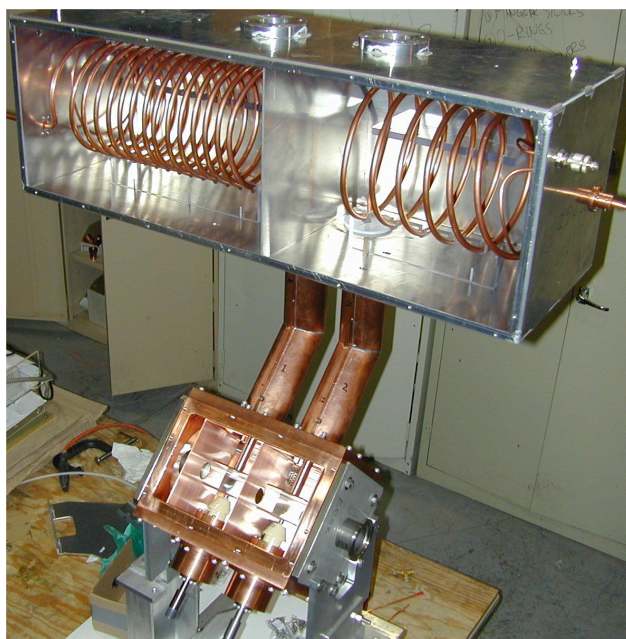


Fig. 144. Dual frequency chopper assembly.

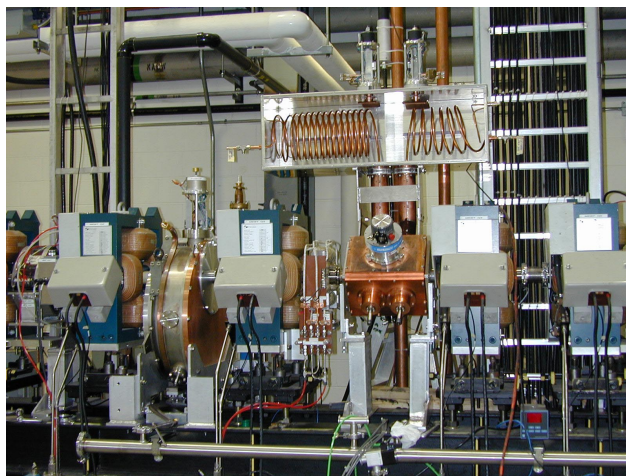


Fig. 145. Bunch rotator and chopper installed in the MEBT.

## Rebuncher

The MEBT 35 MHz rebuncher in general showed sufficiently good performance during beam production this year, though there were a few problems, which gave us some downtime with this device:

- Accelerating voltage instabilities were caused by rf interference from 106 MHz devices located in the same VXI crate. This was overcome with a proper module screening and input signal filtering.
- A capacitive tuner (operating in the frequency automatic feedback loop) failed to move three times (during two months' time). The problem was fixed with a stepper motor control unit replacement.
- Three out of four power modules in the rf amplifier were found to be burnt right before the winter shutdown. The remaining module was just sufficient to provide required rf power for reduced mode of the linac operation ( $A/q = 4$ ).

All troubles most probably were triggered by the unstable operation of the commercial rf amplifier, which could easily fall into parasitic oscillations when loaded with an unmatched high-Q resonant load. In the shutdown, the amplifier will be modified to meet operational conditions.

## DTL

The variable energy DTL is based on five independent, interdigital H-type (IH) structures and three triple gap split ring bunchers, all operating at 106 MHz. All eight DTL resonators are powered by identical 25 kW rf amplifiers developed and assembled at TRIUMF. All systems have been tested up to maximum specified power (see Table XXXI) required for  $A/q = 6$ , but routinely operated mostly at about 4/9 of full power ( $A/q = 4$ ) according to scheduled experiments. The DTL general view is presented in Fig. 146.

### IH tanks

DTL IH rf systems showed very reliable operation during beam commissioning and production this year. The only problem we faced in March, when the system was first commissioned, was that DTL #3 was multipactoring and sparking at high rf levels. The reason was found to be soldering flux trapped in the vacuum pocket behind the downstream hose cone during fabrication (see Fig. 147). Evaporation

of flux in the vacuum volume contaminated tank surfaces and a ceramic window in the coupler. After surface cleaning and nose cone screening with an additional copper electrode, the sparking and multipactoring were suppressed and the tank could stand a maximum specified voltage. But shortly after the problem was resolved, the ceramic rf window broke due to excessive heat dissipated in the deposited layer on the inner surface of the ceramics (see Fig. 148). Another coupler (DTL #1) also came to a critical

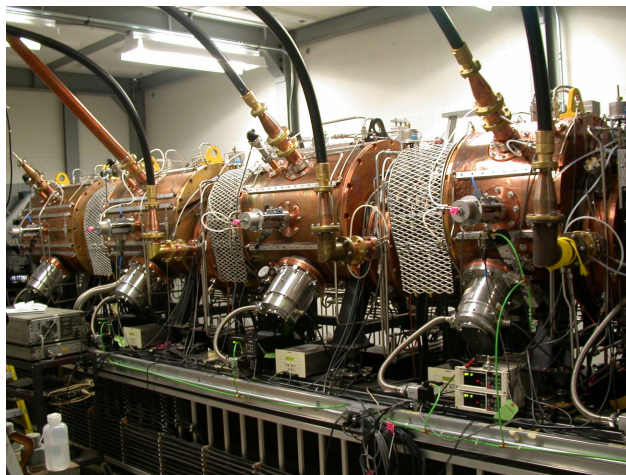


Fig. 146. DTL tanks and bunchers enclosed in the lead shielded bunker.



Fig. 147. DTL #3 nose cone spoiled with a soldering flux.

Table XXXI. Maximum required rf power for DTL systems.

DTL1	BUN1	DTL2	BUN2	DTL3	BUN3	DTL4	DTL5
4 kW	8 kW	10 kW	9 kW	16 kW	12 kW	19 kW	24 kW



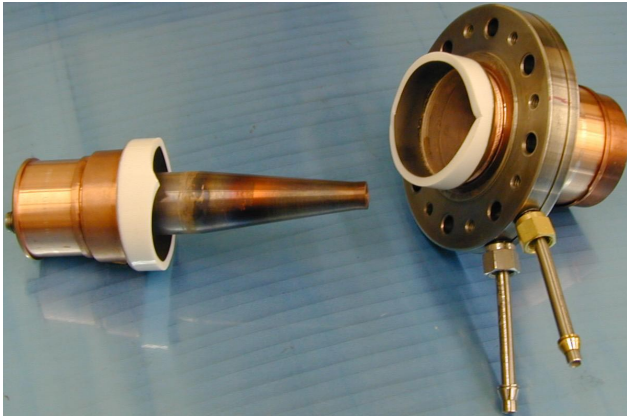


Fig. 148. DTL #3 coupler broken window.

condition. Detailed inspection showed a copper layer spattered all the way around on the coupler inner surfaces. The coupler had been replaced.

During the first year of operation, two powerful rf tubes (4CW25, 000-B) failed, showing grid to cathode short circuit.

### Triple gap bunchers

All DTL bunchers operated reliably during commissioning and beam production phases. The only problem we faced was the failure of buncher #1 power coupler. Detailed inspection showed an aluminum deposition on all inner surfaces of the coupler. Aluminum spattering was very surprising because no aluminum was used in the entire rf structure. The only source for this metal was found to be the  $\text{Al}_2\text{O}_3$  ceramic window, which was indeed eroded due to sparking.

To prevent rf windows from damage in future, two precautionary measures were implemented:

- All the couplers were equipped with infrared temperature sensors.
- High standing wave (VSWR) protection was introduced into the rf interlock.

## HEBT

### Low-beta buncher

The 11.9 MHz low-beta (2.2%) buncher was completed and installed in the HEBT (see Fig. 149) during the September shutdown. It contains two long drift tubes supported with ceramic feedthroughs and two inductive coils located outside the vacuum vessel. The device was successfully tested at full specified voltage of 30 kV requiring only 2 kW of rf power.

### High-beta buncher

The 35 MHz high-beta (3.2%) buncher was commissioned last spring and showed reliable operation in a full range of specified voltages ( $U_{\text{eff}} = 30\text{--}270$  kV).

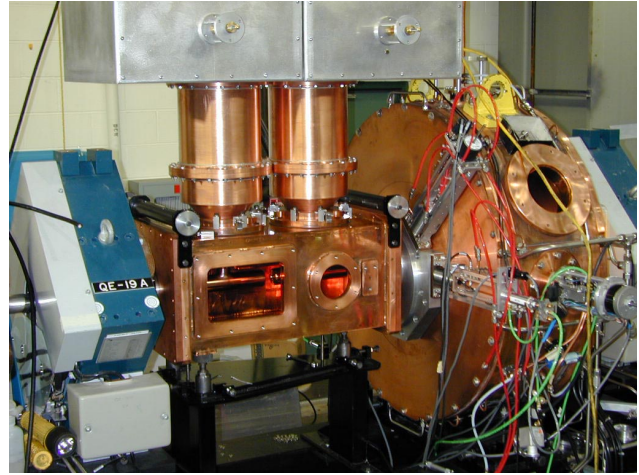


Fig. 149. Low- and high-beta bunchers installed in the HEBT.

Maximum required power is 12 kW. The buncher installed in the HEBT line is shown in Fig. 149.

## ISAC DIAGNOSTICS

### Target Diagnostics

The preseparator diagnostics box DB0 was replaced with one in which the service requirements are more practical. The redesigned DB0 has all mechanics mounted external to the vacuum with independently operated drives for the following devices: slit jaws (left and right) shown in Fig. 150, Faraday cup and scanning wire shown in Fig. 151. For simplicity of the mechanics, the new design utilizes stepping motor drives mounted externally for each of the devices so coupled motions must be done through software. All limit switches are mounted externally. There are no position encoders, the positions are derived by software tracking of the step pulses sent to the motors.

The diagnostics for the east target station (ITE) were designed, and much of the work completed, by year-end. The east target station is to be operational by the spring of 2002 so installation work will be done during the winter shutdown. Three new proton beam monitors will be installed – two for ITE and an additional one for ITW. The diagnostics in the ITE entrance module are identical to those in ITW; they were completed and mounted on the module in December. The mechanics for the ITE exit modules devices required redesign. Most of the parts were ready by year-end; assembly and installation is to be done early in the winter shutdown. ITE:harp5B was built and ready for installation early in the new year.

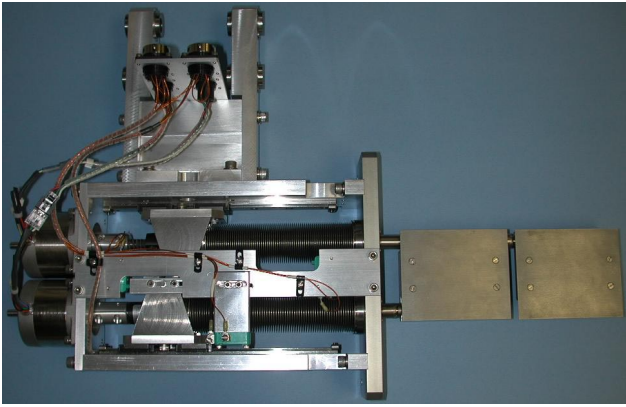


Fig. 150. DB0 slit assembly.

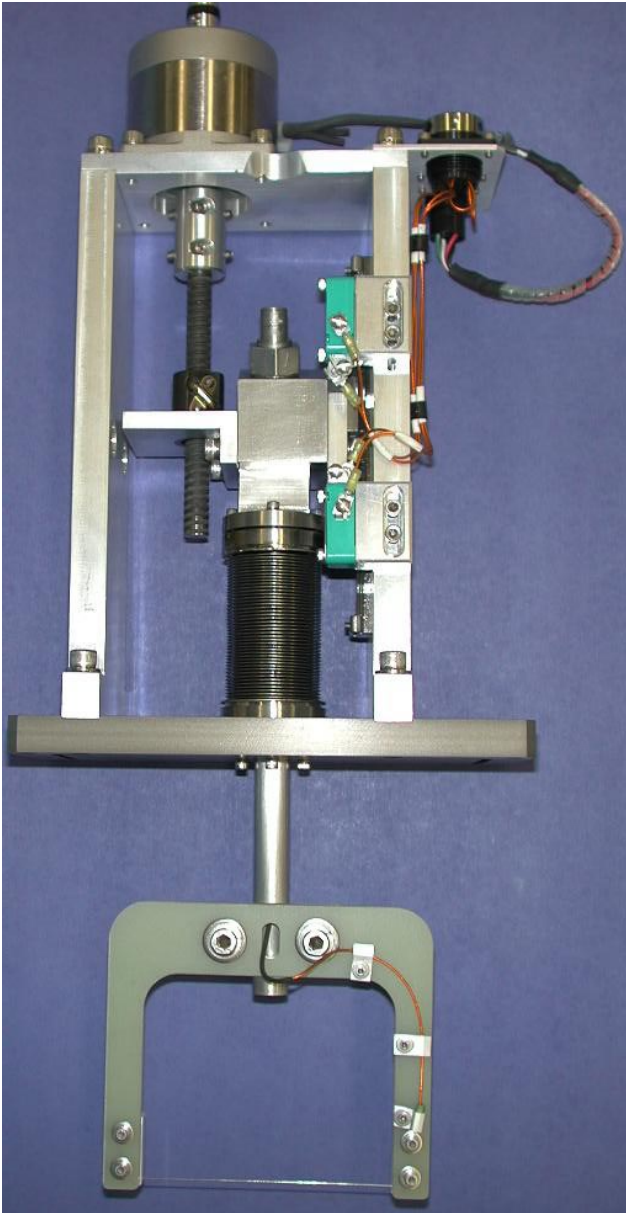


Fig. 151. DB0 wire scanner assembly.

## MRO

Mounting techniques were developed for a variety of foil types procured for the MEBT stripping foils. A working space was equipped in the ISAC cold chemistry lab and a significant effort was devoted to providing foils as needed for commissioning and operation. The diagnostics electronics support provided electronics modules, cabling and system integration for the diagnostics of the new ISAC installations of HEBT and TUDA. ISAC development projects included the installation of a multi-position beam attenuator, a channeltron, and other devices such as fast Faraday cups and wire scanners.

## Waste beam monitor

A system has been developed to continuously monitor the flux of radioactive ions. It consists of a 2.25 in.<sup>3</sup> BC412 plastic scintillator placed below the vacuum chamber in MEBT that contains the charge selection slits. It responds to the  $\gamma$ - and energetic X-rays produced when the unwanted charge states decay to more stable isotopes. The states neighbouring the desired mass are dispersed by the MEBT bending magnet and hit the slits or the beam pipe between the two. The flux of neighbouring masses should mimic the flux of the mass selected when the ion source, accelerator or stripping foil parameters change. The PMT output is discriminated, level converted and passed to a VME scalar. The rate is displayed via the EPICS system.

## Cables

A variety of different cables have been laid to the five diagnostics stations in the HEBT, DRAGON and TUDA lines. These should assist with the timely provision of special monitors and the development of diagnostics.

## Silicon detectors

Silicon detectors have been used in conjunction with scattering foils in two different applications. The first provided an extra calibration of a momentum spectrometer, the Prague magnet, using known resonances in the  $^{12}\text{C}-\alpha$  elastic scattering excitation function. The geometry is shown in Fig. 152. The target consisted of a  $20\ \mu\text{g}/\text{cm}^2$  layer of gold evaporated on the upstream side of a  $20\ \mu\text{g}/\text{cm}^2$  layer of carbon and was placed at  $45^\circ$  to the beam. The scattering angle of  $98^\circ$  is close to the optimum of  $105^\circ$ . The amplifiers and MCA were calibrated using a three-component  $\alpha$  source. The energy measured from elastic scattering of  $\alpha$ s from gold agreed with the nominal 1 MeV/u after corrections for kinematics and energy loss in the target. The lower energy elastic peak from carbon was quite clean when the beam was well tuned. The total

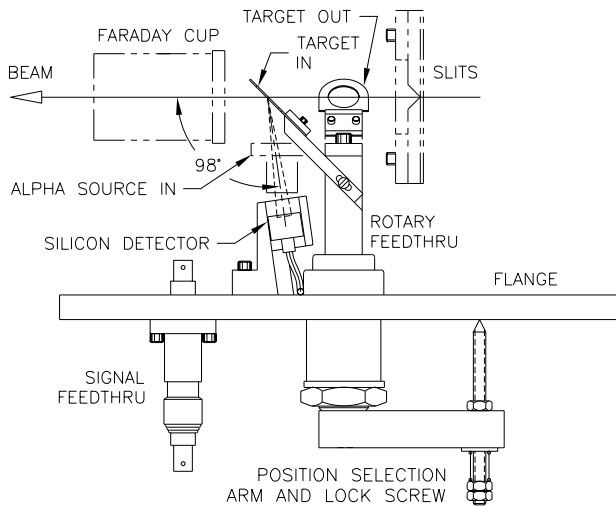


Fig. 152. The target holder can be rotated to one of three positions. One position places the foil in the beam path, the second places an alpha source in front of the detector, and the last is blank.

number of counts in the peak at 3.82 MeV, from the 4.256 resonance, was recorded as the nominal helium beam energy was varied between 4.05 and 4.5 MeV. The results were normalized using the counts in the gold peak since we did not have a digitized Faraday cup signal synchronized with the data acquisition. The resonance edge could be seen clearly and implied, after correction for small losses in the target, a beam energy  $\sim 20$  keV higher than that inferred from the magnet setting.

The second application measured the distribution in time of the ion beam and was used to optimize the setting of the rf bunchers. Particles were scattered into a 50 mm<sup>2</sup> Canberra PIPS detector from a gold target supported on a thin carbon foil. A 2003BT Canberra pre-amplifier was used most of the time and the E and T signals sent to linear and timing filter amplifiers (TFA) respectively. The TFA output passed through a CFD to provide the start signal for a time-to-pulse-height converter. The stop signal was obtained using a discriminator to transform the fundamental 11.67 sine wave from the accelerator rf synthesizer into a train of NIM pulses and then halving that frequency. The data could be displayed in correlated E-T (i.e. E- $\phi$ ) form or as a 1-D time distribution. Bunch widths as low as 0.95 ns FWHM were measured and the energy resolution was  $\sim 22$  keV. The 2-dimensional display showed tightly bunched distributions in the buckets expected for various chopper and buncher modes. Particles only fell outside the buckets when devices were grossly mistuned. This meant that the easier to set up 1-D display could be used for optimization of stable beams. The decay products of radioactive ions scattered into the detector will be registered along with the primary ion. The former will not be correlated with the rf clock and

could form a continuous background. Silicon detectors, as opposed to secondary electron based detectors such as MCPs, do not give a large response to electrons and photons but do record  $\alpha$  and other ion emission. An E-T display from a  $^8\text{Li}$  beam showed the scatter of decay products but the narrow primary beam peaks stood out sufficiently from the background that 1-D displays could be used for tuning. The latter will be displayed via EPICS using a VME TDC.

An associated benefit is the use of the ion count rate and the known Rutherford cross sections to estimate beam current at levels below the response of a Faraday cup.

The resolution is sufficient for tuning purposes. Better resolution was obtained for 1-D distributions by using a ZKL-2R5 Mini-Circuits pre-amp. Further improvements could be achieved, at the cost of an increased background, by using an MCP. Both the count rate per pA and the time resolution would be improved by scattering at more forward angles. This requires optimizing the layout of this apparatus with other diagnostic equipment.

#### Beam attenuator

A compact arrangement of meshes, or sieves, has been placed in box IOS DB7 in order to attenuate the stable beam current from levels suitable for tuning the accelerators and beam lines to levels tolerable to particle detectors. There are 5 rods 1.5 in. apart operated by air cylinders with speed reducers. Each rod carries one screen. Most laboratories place two sets of attenuators sufficiently far apart that the beam emerging from each hole in the first set expands to cover the mesh structure of the second. Having all meshes in one box means that the aperture size and spacing of the rear-most grids must be scaled down by the drift ratio of, say, 1 m to 75 mm. We use drilled copper plate or commercial wire sieves on the front pistons both to supply small changes in beam flux and to absorb any high wattage. Commercial nickel sieve material with 5  $\mu\text{m}$  holes spaced 50  $\mu\text{m}$  and polycarbonate filters with a random distribution of 5, 8 or 12  $\mu\text{m}$  holes are used for the rear rods. Several filters with random distributions may be stacked to give high degrees of attenuation. Reduction factors of 10 to 4000 have been measured for single screens and higher factors have been obtained with combinations. The reduction factor varied by less than 6% as an  $^{16}\text{O}^+$  beam was steered over the surfaces and the expected ratio agreed with the measured ratio to a similar precision.

The recalibration will be repeated periodically to check that the finer screens are not deteriorating due to beam exposure, either radiation damage or holes being covered by fragments of oil or dirt drifting up or down the beam pipe.

## Danfysik emittance rig upgrade

The Danfysik emittance rig consists of a profile monitor placed about 0.5 m downstream of a slit. The two move stepwise across the beam together. The rig had been moved downstream of the DTL, just ahead of the Prague magnet. At the same time, the electronics were upgraded from a dc amplifier-per-channel system to a scanning charge integrator system using a VICA 96 VME module. The Danfysik profile monitor is an array of metal lines etched on a solid insulating substrate, however, and beam deposition had led to electrical conduction between adjacent lines. The effect of this leakage had been reduced in the dc amplifiers by using very low offset op amps to reduce the line-to-line voltages. With the new system it was found that the voltages produced across the input capacitors as the charges accumulated led to excessive leakage through the deposition. The substrate was replaced with a new harp consisting of fifteen 0.005 in. diameter Au plated Mo wires spaced 0.8 mm apart supported in vacuum by a G10 frame. This eliminated the leakage and with the charge integrator system it was possible to obtain an emittance measurement using a 1 nA  $O^{+4}$  beam using a dwell time of 800 ms. The dwell time is the time during which the motion of the slit pauses for each complete profile measurement. The new system permits long integration times of the current collected by the harp wires and the dwell time may be increased proportionately. It was possible to obtain a very clean emittance scan for a 25 epA beam using a dwell time of 4 s and background subtraction

## RF multiplexer

A solid state rf multiplexer has been developed. It has a wide bandwidth from 4 MHz to 5 GHz and can be controlled by GPIB or through Ethernet via an adapter. It will be used with oscilloscopes and phase meters to increase the number of inputs.

## Phase probe

A non-intercepting pickup was installed in the diagnostics box in front of the high-beta buncher. It is a narrow band device, resonant at the fourth harmonic of the bunch frequency, 47.5 MHz, with a loaded Q of 200. The sensitivity was measured using a 50 nA beam of  $^{16}O^{+4}$  and was found to be  $0.9 \mu V_{RMS}/nA$ . The phase jitter of the beam with respect to the rf system synthesizer was measured using an HP8508A vector voltmeter. The result was  $\pm 2^\circ$  at 47.5 MHz. A jitter of  $\pm 1^\circ$  can be achieved with 10 nA of beam by adding a pre-amp.

## Stripline FFC

The 50  $\Omega$  cone type fast Faraday cups in use in the MEBT and HEBT lines are too long in the beam di-

rection for use in the diagnostic boxes of the DTL. An assembly drawing of a short stripline type cup for use there has been made.

## BEAM COMMISSIONING

### MEBT

The MEBT optics and rf devices have been fully commissioned with beam. A bunch rotator and chopper are installed upstream of the stripping foil. The 106 MHz split ring bunch rotator is the slightly modified prototype buncher for the DTL. It provides a time-focus of the beam on the stripping foil to reduce the emittance growth due to energy straggling. The device results in improved capture by the DTL and reduced longitudinal emittance at the experiment.

The chopper has two modes of operation, one giving a bunch spacing of 85 ns removing 5% of the beam, and the other a bunch spacing of 170 ns that removes 53% of the beam. The chopper consists of a series of two sets of plates located where horizontal divergence has been minimized followed by selecting slits near the stripping foil  $\sim 90^\circ$  phase advance downstream. Each plate pair has one plate driven at rf voltage (11.8 MHz and 5.9 MHz respectively) and the other compensating plate is dc biased to produce zero deflecting field at the base of the rf waveform to reduce transverse emittance growth. In the first mode the two 35.4 MHz side-bands in the pulse structure (Fig. 153(d)) are deflected at 11.8 MHz (Fig. 153(a)) yielding the time structure shown in Fig. 153(e). In the second mode the side-bands plus every second main pulse are deflected by adding the 5.9 MHz deflection (Fig. 153(b)) from the second set of plates to yield the combined deflecting field shown in Fig. 153(c) giving the time structure measured in Fig. 153(f).

Beam simulations show that such a chopper should not increase either the transverse or longitudinal emittance. Two lumped circuits drive the rf voltage on the plates up to  $\sim 7$  kV each. The chopper is now operational and proves very reliable and easy to tune. A profile monitor at the chopper slit is used to record beam deflection and to optimize the chopper phase and then the dc bias is set to optimize transmission through the chopper slit.

### Full DTL Beam Tests

The full DTL was installed in the latter half of 2000 (Fig. 154) with the first beam accelerated to full ISAC energy of 1.53 MeV/u on December 21, 2000.

Beam commissioning in January, 2001 with the complete DTL using  $^4He^{1+}$  beams established the DTL rf parameters and beam optics settings for over twenty different energy set-points covering the full specified operation range. Initial phase and amplitude set points



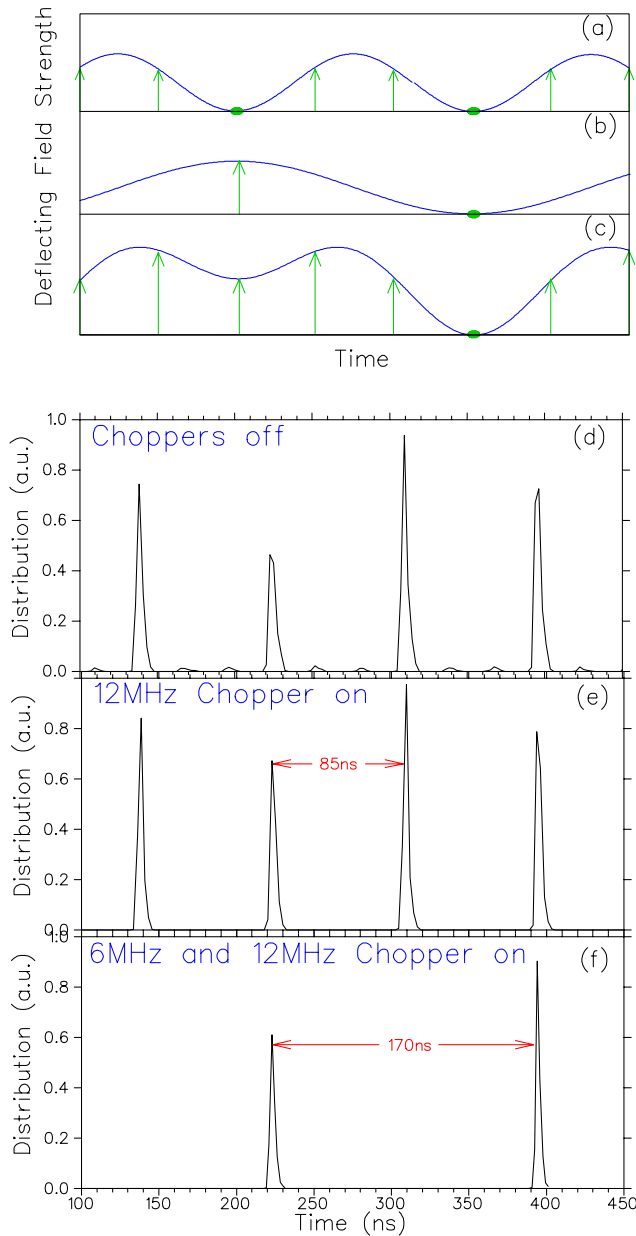


Fig. 153. Output time structure from the RFQ is shown in (d). The field produced by the 11.8 MHz chopper plate (a) produces an 85 ns time structure shown in (e). The field produced by the 5.9 MHz plate in (b) is combined with the 11.8 MHz deflection to produce the combined deflection shown in (c) and generates the time structure given in (f).

are determined empirically by beam energy measurement; each accelerator component is turned on and optimized sequentially before advancing to the next device. The DTL triplets are adjusted to optimize transmission with each large energy step.

The transmission through the DTL was over 95% for all cases. A summary plot of the accelerated beams is given in Fig. 155.

Longitudinal beam quality for all beams is as predicted. Sample spectra and associated pulse width 5 m

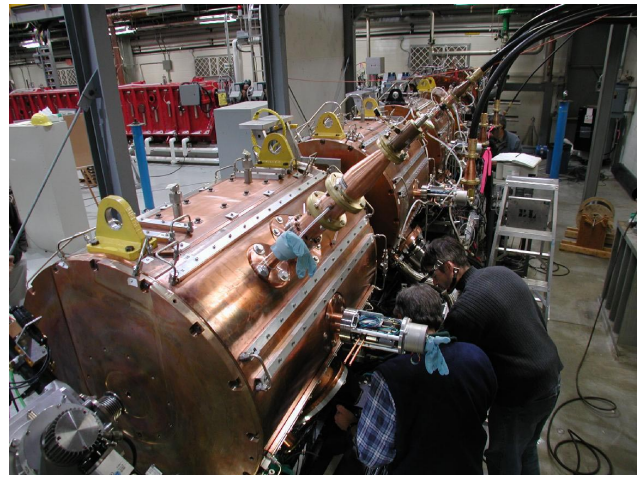


Fig. 154. The ISAC 106 MHz DTL.

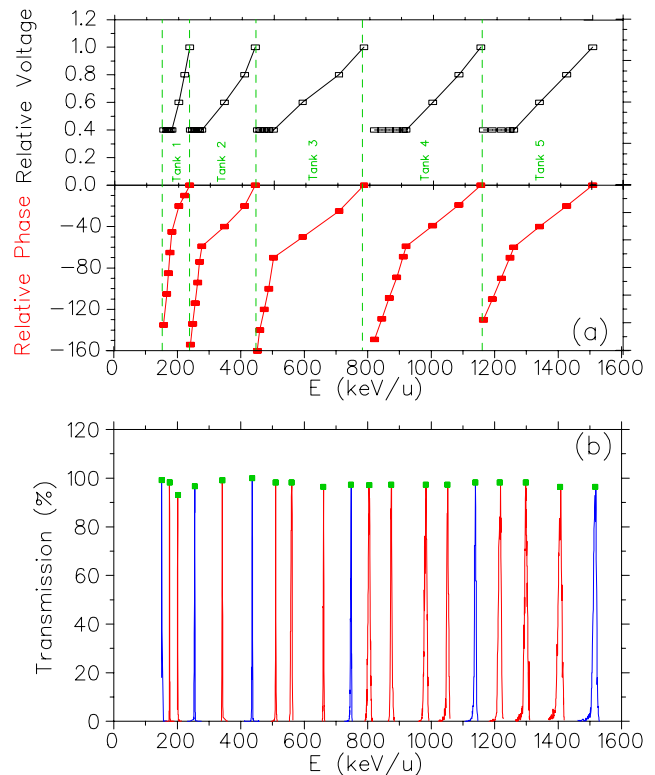


Fig. 155. Shown in (a) are the DTL rf set-points established through beam simulation. In (b) we plot the measured transmission for the various beams that have been accelerated through the DTL during commissioning studies with  $^4\text{He}$ .

downstream of the DTL are recorded for a wide range of energies corresponding to both conditions where the last operating tank is operating at the design voltage, Fig. 156, and conditions where the last operating tank is at a detuned voltage, Fig. 157.

#### Final energy

The ISAC DTL is designed for a maximum energy of 1.53 MeV/u and for a maximum  $A/q = 6$ . The

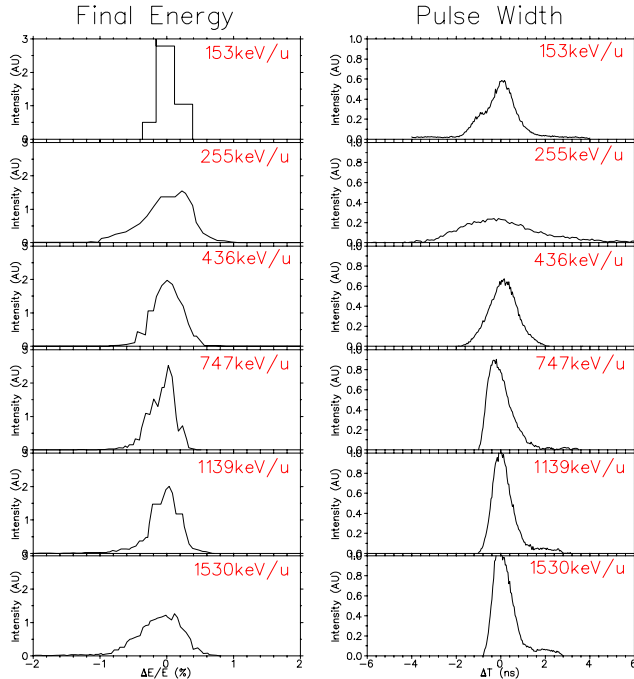


Fig. 156. A sample of energy spectra and associated pulse width measured 5 m from the DTL for tanks operating at design voltage.

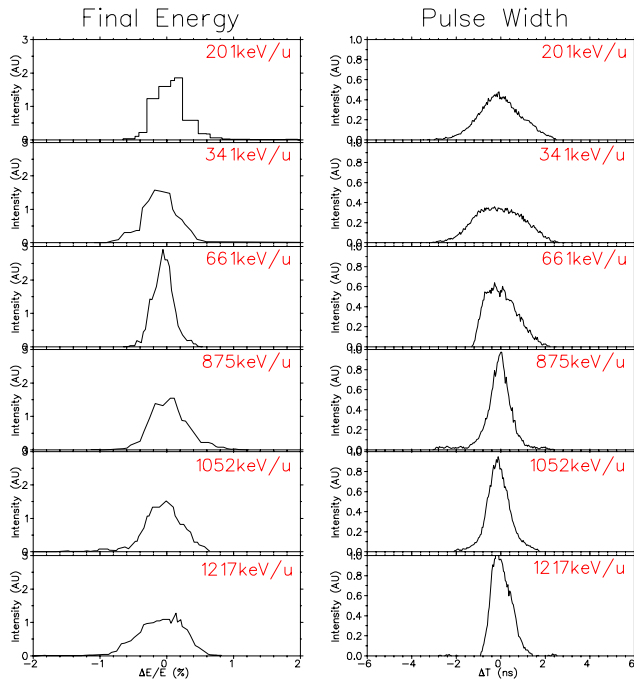


Fig. 157. A sample of energy spectra and associated pulse width measured 5 m from the DTL for the last tank operating at a detuned voltage.

DTL essentially operates as a fixed velocity accelerator with voltage and phase detuning in the last operating tank to accelerate to a reduced energy. The full energy range from 0.153–1.53 MeV/u can be spanned by this method. Conversely it is possible to reach a higher

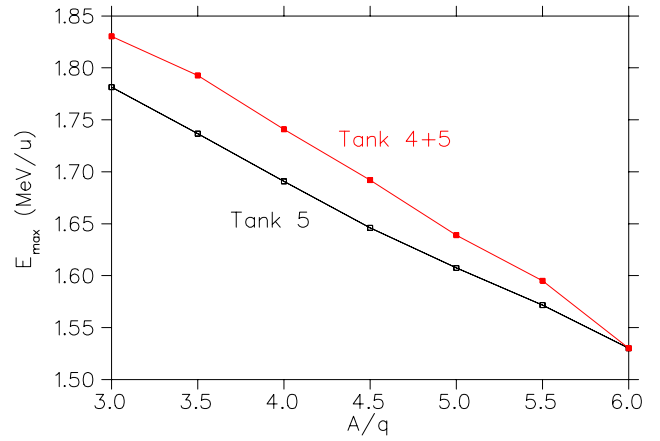


Fig. 158. Final beam energy simulated for two cases. In the first case Tank 5 voltage is operated at maximum and the phase is altered to maximize the acceleration. In the second case both Tank 4 and Tank 5 are maintained at maximum voltage.

final energy than specified by increasing the voltage in the last operating tank and optimizing the phase for maximum acceleration. Assuming that the maximum voltage in a tank occurs for  $A/q = 6$ , then these higher energies are only possible for  $A/q < 6$  values. Since the higher voltage increases the particle velocity above the design value, phase slippage during the tank crossing occurs. Therefore as the relative voltage increases, the incident particles must be pushed to more and more positive phases to achieve maximum acceleration. Some additional energy can be achieved by increasing the relative voltage on the second to last tank to maximize the energy entering the last tank. The gain cannot be duplicated by increasing the voltage in all tanks since the large phase slip caused by accelerating particles with a velocity higher than designed does degrade longitudinal beam quality. Simulated final energies for two cases, one where Tank 5 alone is increased in voltage, or the second where both Tank 4 and Tank 5 are used, are given in Fig. 158.

### HEBT

The high energy beam transport (HEBT) feeds two target stations 23 m and 30 m downstream of the DTL: the DRAGON windowless gas target and recoil mass spectrometer, and the TUDA multi-purpose detector array. The HEBT is composed of four basic sections: a section to match the beam from the DTL to the HEBT, a diagnostic section and bunching section, achromatic bend sections to deliver beams to the experiments and matching sections to focus the beam to the experimental targets.

The diagnostic section is used by accelerator personnel for beam commissioning and pre-tuning before experiments. Included in the section are a high dispersion  $90^\circ$  analyzing magnet for beam energy and en-

ergy spread analysis and a transverse emittance rig. A low- $\beta$  ( $\beta_0 = 0.022$ ) 11.8 MHz rebuncher and a high- $\beta$  ( $\beta_0 = 0.032$ ) 35.4 MHz rebuncher are positioned on either side of a double focus positioned 12 m downstream of the DTL. The 11.8 MHz rebuncher is a three-gap structure driven by two lumped element circuits with up to 30 kV required on each drift tube. The 35.4 MHz buncher is a two-gap spiral device similar to the MEBT rebuncher with up to 170 kV required on the drift tube.

The HEBT line including the high- $\beta$  buncher has been commissioned in April, 2001. Figure 159 shows the beam time distribution close to the DRAGON target for the buncher off and on. The low- $\beta$  buncher has been commissioned in September, 2001. Both bunchers perform as specified giving the flexibility to adequately bunch the beam over the whole energy range of the DTL.

## Beam Delivery

### Stable beams

Stable beams of  ${}^4\text{He}^{1+}$ ,  ${}^6\text{Li}^{2+}$ ,  ${}^{13}\text{C}^{3+}$ ,  ${}^{14,15}\text{N}^{4+}$ ,  ${}^{16}\text{O}^{4+}$ ,  ${}^{21}\text{Ne}^{5+}$ , and  ${}^{24}\text{Mg}^{6+}$  have been delivered to the two experimental facilities at various beam energies. The early stable beam delivery periods proved essential both in training the operators and in determining hardware improvements and required developments prior to first scheduled radioactive beam delivery of  ${}^8\text{Li}$  in mid July. Although the ISAC DTL is a variable energy device, it still essentially operates as a fixed velocity linac (except for the last operating tank) so that phase relationships between cavities are fixed regardless of particle mass and charge and only the voltage need be scaled, shortening beam tuning time. Small energy steps down to 0.1% are easily realized by linear voltage or phase steps in the last operating DTL tank. New beam tunes are established by a beam physicist with round the clock delivery by ISAC operations staff. The ISAC operators have quickly adjusted to the new

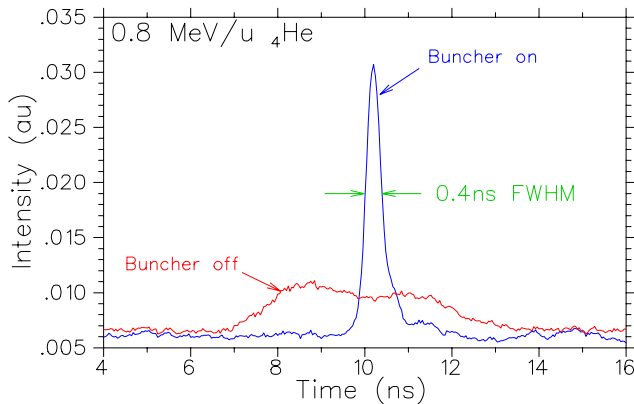


Fig. 159. Beam time distributions measured on a fast Faraday cup near the DRAGON target for high- $\beta$  buncher off and on.

accelerators and now handle routine procedures such as foil changes, energy changes and recovering beam delivery after hardware trips.

Several early improvements have been added that greatly reduce linac tuning time. Foil changes are facilitated by a global phase shifter between the pre-stripper and post-stripper accelerator sections to account for slight differences in foil thickness. A cold trap surrounding the stripper foil has now minimized foil thickness changes and lifetime issues due to carbon build-up.

### Radioactive beams

The first radioactive beam to be accelerated at ISAC was  ${}^8\text{Li}^{2+}$  delivered to the TOJA facility that occupied the target location on the TUDA line. This first run was instrumental in establishing operational procedures to deliver radioactive beams to target. The beam delivery starts first by choosing a stable pilot beam from OLIS with the same  $A/q$  as the radioactive beam for both the pre-stripper and post-stripper lines. In the case of  ${}^8\text{Li}^{2+}$ , we used  ${}^{16}\text{O}^{2+}$  from the source and  ${}^{16}\text{O}^{4+}$  in the post-stripper section as the pilot beam. The beam tune is established and optimized to the correct energy and delivered to the experiment. In parallel, the radioactive beam is optimized through the mass separator and low energy optics transport. Once both beams are established it is straightforward to switch from stable to radioactive beams. The low energy bend electrode in the switchyard is switched to change the beam path from OLIS to the mass-separated beam. Next the optics and steering in the switchyard section are optimized to match the radioactive beam to the accelerator. This is done by maximizing the beam to a Faraday cup just upstream of the RFQ. Since the stable beam and the active beam come from different platforms there is a small energy difference between beams so a phase shifter is used to optimize the phase of the beam entering the RFQ by maximizing the accelerated beam to the stripper foil box. Lastly the beam is sent through the DTL to experiment. The global phase shifter between RFQ and DTL can be used to cancel any differences between the interaction of the pilot beam and the radioactive beam in the stripping foil.

At present the radioactive beams are mostly tuned by standard high intensity diagnostics including Faraday cups and scanning wire profile monitors. A low intensity timing diagnostic consisting of a gold foil and silicon detector was added upstream of the TUDA facility to help tune the buncher for low-intensity beams. A multi-head pepperpot device was added after OLIS that can change the intensity of the stable beam by several orders of magnitude. This is very useful to aid

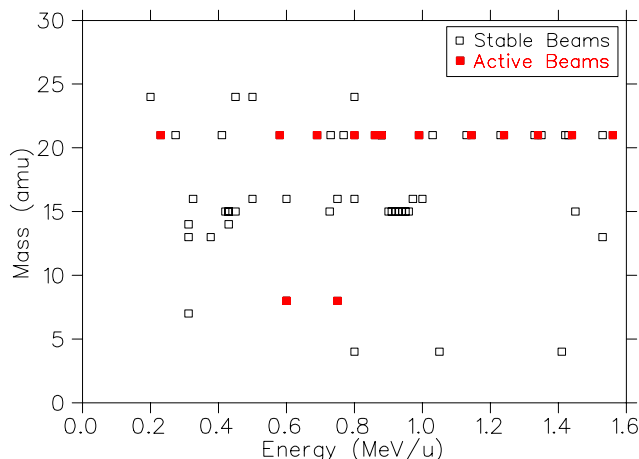


Fig. 160. A summary of stable and radioactive accelerated beams delivered to experiment in 2000.

in tuning through experimental target chambers where damage to detectors is a concern.

A summary of the stable and radioactive beams delivered to experiment in 2000 is shown in Fig. 160.

## LEBT

Four new beam lines have been constructed this year as extensions to the LEBT section of ISAC. They are: GPS1,  $8\pi$ , polarized beam lines polarimeter, and Osaka.

### GPS1

The general purpose station (GPS) has been relocated to the northwest corner of the LEBT area to facilitate the installation of  $8\pi$  in this location, and has been re-designated as GPS1. In order to accomplish this relocation, the beam line was extended 2 m to avoid interference with polarizer equipment. Four new electrostatic quadrupoles were added for beam transport purposes. The beam line will be commissioned in early 2002.

### $8\pi$

The  $8\pi$  beam line was designed to bring the beam to the  $8\pi$  spectrometer. This line is the longest extension added this year to the LEBT with one  $45^\circ$  electrostatic bend, twelve electrostatic quadrupoles, two pairs of  $x$  and  $y$  slits, four emittance scanners, and three Faraday cups. The vacuum system consists of two independent sections pumped by turbo molecular pumps with fore pumps for each section.

The beam line was installed and commissioned in November, 2001 with stable beam from the off-line ion source (OLIS).

### Polarimeter

The polarimeter system was designed for nuclear polarization measurements of an ion beam emanat-

ing from the polarizer. The design incorporates an ultra high vacuum system for future experiments using low-magnetic-field  $\beta$ -NMR at cryogenic temperatures on the target. The UHV system operates at  $1.2 \times 10^{-10}$  torr and consists of three vacuum chambers pumped by two 500 l/s turbo molecular pumps, and one 1000 l/s cryopump. The ion beam is focused onto a stopper foil (target) placed in the centre of the last chamber, where the nuclear polarization is measured by observing the beta-decay asymmetry with plastic scintillator telescopes placed outside the chamber. Helmholtz coils provide a magnetic field of up to 0.02 T to maintain nuclear polarization. The polarimeter system also can be used for other experiments with minor modifications or extensions. The polarimeter was commissioned in August, 2001, and has successfully measured the polarization of  $^8\text{Li}$  and  $^9\text{Li}$  beams.

### Osaka

The Osaka beam line is another extension of the polarized section of LEBT and is designated as a general purpose facility for polarized beams. The line has been designed and named for the first experiment on it – Expt. 903: Professor Shimoda’s group from Osaka University. Their run is planned in 2002 with polarized  $^{11}\text{Li}$  beam.

The line includes one  $45^\circ$  electrostatic bend, nine electrostatic quadrupoles, two emittance scanners, and a Faraday cup. The Osaka beam line vacuum system is an extension of a section between the polarizer and  $\beta$ -NMR. It is pumped by a turbo molecular pump installed on the bend box in addition to the existing turbo molecular pump with the roughing-backing collector extended from the existing fore pump.

The Osaka beam line should be commissioned in early 2002.

## MASS SEPARATOR

During 2001 the ISAC facility delivered several radioactive ion beams. Even though the commissioning of the mass separator was never completed due to lack of time, we were able to tune the beam with sufficient reliability over the year. The highlight is the complete separation of  $^{75}\text{Ga}$  and  $^{75}\text{Rb}$ . The mass difference is only  $1.61 \times 10^{-4}$ , which corresponds to a resolving power larger than 6000.

During the year several users reported beam intensity instabilities that look like a rapid decrease and a slow recovery. We monitor the beam intensity on a Faraday cup just after the mass separator over several hours without seeing any instability except for high voltage sparks which show a fast decrease and rapid recovery. The investigation will continue during this shutdown period.



During the 2001 winter shutdown period we worked on the high voltage Faraday cage around the mass separator and proceeded to the installation of the insulation transformer and high voltage power supply.

During the 2002 winter shutdown period we will finish the installation of the services and the safety equipment for operation under high voltage conditions and in March we have three weeks scheduled for commissioning of the mass separator and the high voltage platform.

## EAST TARGET STATION

In January, a decision was made to complete the east target station to be operational by the spring of 2002 as a top priority for ISAC. Previous to this, the main effort was directed towards supporting the operation of the west target station, completing many unfinished tasks in the target hall, remote handling, building spare target modules (TM2) in case of problems with TM1 in service, and TM3 to house the ECR source that was in development, to be completed later in 2001. In order to achieve completion of the east target station, the project was broken down into work packages and schedules. The major work packages with a brief description are as follows:

### Modules

It was realized at this time that removal of the TM1 containment box tray (supporting the surface source extraction column) remotely in the hot cell was not possible due to interference between the extraction column and the services from the service duct (i.e. H<sub>2</sub>O lines and conductors). TM1 at that time had not accumulated much radioactivity and this deficiency was corrected with a hands-on modification outside of the hot cell. It was also realized that providing services (down the service duct) for an ECR source (TM3) could not be dealt with in the same way due to the greater number of conductors and increased complexity of the extraction column.

In order to ensure that the containment box tray supporting the extraction column and/or the service tray can be removed from the target module in the hot cell, the entire service philosophy was revisited. This resulted in an intensive design study which introduced the use of 14 water block/current connectors allowing all services from the containment box tray to be disconnected from those coming down the service tray, allowing for both tray removals. Special tooling and fixtures were designed to allow this complex procedure to be accomplished in the hot cell by manipulators. The simpler surface source uses only those water blocks necessary, hence the target module now caters to either source. This redesign work was timely since progress on the design of the ECR had been delayed and now

a more coordinated approach could be employed. This was particularly true regarding the ECR waveguide, details of which proved to be an engineering challenge in order to accommodate it through the shield plug and interface with the HV ECR cavity through a choke.

When TM1 was redesigned to produce TM2 (etc.) the reason was to improve accessibility to the service duct as well as simplify many aspects of the design and also improve manufacturability. It was also the intention to utilize the same design for the EXIT modules for the east target station. This, coupled with a new optics design for both EXIT modules, required considerable redesign of the service cap, service duct contents, containment box and contents, as well as the optics themselves and all linkages and actuators for the diagnostics.

The entrance and dump modules required no fundamental changes other than the fact that they are mirror images of the west station due to the proton beam offset relative to the centre of the module. Hence a new set of drawings was required and there is no interchangeability with the west station.

### 2A beam line

Work had commenced on the design of the 2A switching magnet (2AB3) early in 2000. The schedule for manufacture, delivery, mapping, etc., allowed for a timely installation to meet the east target station schedule. The remainder of the beam line 2A3 to the east target station mimicked that of the west station and therefore required the ordering and manufacture of components ready for installation, which could only commence during the shutdown (i.e. 2002).

### East module access area (EMAA)

(Note: This area is actually the volume below the shield plugs and above the vacuum tank.)

At the beginning of this report period the east target tank had been installed and aligned and no further action had taken place. In February, this work package was planned and a schedule was drawn up to complete all work necessary to render the east station operational in May, 2002.

The EMAA work package included:

- EMAA preparation. This work involved completion of the diaphragm air sealing system which is part of the overall nuclear ventilation system, completion of the 5b shielding package between the east tank and the preseparator magnet, installation of the east tank top plate and seal (and check for leaks), installation of the upstream proton beam window and window shield plug, etc., and installation of the inter modular connector (IMC). This is a pneumatically actuated capsule

that is installed in the tank at 3 locations and connects the target/EX1/EX2 modules together and then to the RIB exit beam line to separate primary from secondary vacuum to minimize potential contamination.

- EMEA layout. In order to maximize accessibility (and minimize dose), installation of all services such as cabling, air lines, vacuum lines, H<sub>2</sub>O lines, cable trays, etc., is controlled by an installation layout which is supervised by the target hall coordinator. An ECR source (TM3) requires installation of a 2.45 GHz waveguide to connect to the module waveguide flange at the top of the service cap. It was decided that the best arrangement would be to install the power supply and generator in the electrical room, and then the magnatron, isolator, and autotuner would be located in the EMEA. These items required attention to provide the location and support necessary, and designed such that a piece of waveguide could be detached quickly for module removal.

## Services

At the time of installation of the west target station, none of the services were extended to the east target station. However, the H<sub>2</sub>O and vacuum systems are sized to handle both. Due to operational requirements, both systems required modifications to allow the non-operational station to condition targets (i.e. H<sub>2</sub>O and vacuum required). These systems were designed and installation commenced in the fall. High voltage services from the electrical room Faraday cage would mimic those of the west station, but installation could not commence until the shutdown (January, 2002). The HV containment chase had been prepared previously. There were two grounding circuits required to be installed from the electrical room through the HV chase and EMEA, to the preseparator area and to the mass separator. One is a heavy cable for building ground, and the other rf type ground to deal with the eventuality of a HV spark over. These will be dealt with as construction and installation progress.

## Faraday Cage and Electrical Room

As mentioned, nothing had been done to provide high voltage services to the east target station prior to 2001, and construction work in the electrical room was only allowed when the west station was not operating. During the year, construction was scheduled to take advantage of maintenance days, and target change shutdowns to conduct the Faraday cage, necessary services, cable trays and electronics racks. All required power supplies, transformers, controllers, etc., were ordered early in the year.

## Other Systems

Information regarding the control system related to proton beam, radioactive ion beam, and target protect, are found elsewhere in this Annual Report under Controls. Safety systems related to the east target station can be found in this Annual Report under Operational Safety. This describes the philosophy of the safety interlock system. Operation of the west target station has shown that radiation emanating from the H<sub>2</sub>O package and transport piping is too high and requires shielding (as was expected initially). The H<sub>2</sub>O package currently has shielding but there are too many shine paths. This was inspected and a proposal approved by the Safety group. Installation will commence in 2002.

## ISAC PLANNING

This year the Planning group was involved in planning, scheduling, coordinating and expediting several sub-projects for ISAC.

Various plans and PERTs were prepared and updated regularly with manpower estimates and analysis to identify critical areas and resolve any problems. ISAC priorities were evaluated and higher priority was assigned to: the east target station with an aim to install in the winter, 2002 shutdown and optimize RIB operation for the ISAC experimental program; expedite the low energy experimental program that included a first data run at  $\beta$ -NMR; move GPS1; Osaka beam line; and commission TUDA and DRAGON with stable beams and RIB.

On the accelerator side, major milestones (after beam to 1.5 MeV/u in December, 2000) included installing and commissioning the 11 MHz buncher by September to facilitate commissioning of high energy experiments (TOJA, TUDA and DRAGON) by November. Manpower planning was done, activities were coordinated and expedited, and the above goals were achieved on schedule.

Technical details and progress on PERTed activities are described elsewhere in this report under the respective principal group. However, following is a summary of the main projects along with the major milestones achieved.

## East Target Station

This project received high priority and had to be fast-tracked for installation in the January, 2002 shutdown. The project was broken down into 9 work packages that included: 2A beam line, IMC, MAA, Faraday cage, target hall, services, controls, safety, and 5 target modules (entrance, dump, exit 1 and 2, and target module). Major highlights of these work packages included: 2A beam line (switching dipole received in September, monitors and associated beam line hardware received in December), Faraday cage (constructed

by July and isolation transformer, high voltage and other power supplies procured by October), target hall (including modification and commissioning of south hot cell and storage silos in July, alignment components and water packing shielding in November), controls (including 2A controls, target protect interlocks and RIB controls for vacuum system, beam optics and beam diagnostic systems). Work on modules was a major work package that required extensive Design Office and Machine Shop effort. Several design modifications were made for better manufacturability and handleability. Shield plugs were ordered in April, with a staged delivery for most modules in July. Below is a summary of the modules work packages:

- Dump module included shield plug dump and pipes which were designed by the University of Victoria engineering group and fabricated in October. Entrance module included shield plugs, diagnostics (2A 3M19, M20, collimator) and associated electronics.
- Exit modules 1 and 2 included shield plugs, containment boxes, service and pumping ducts, service caps, optics (water-cooled), diagnostics (collimator 3 and harp 3 for exit 1, and collimator 5, harps 5A, 5B and Faraday cup).
- Target module required extensive design changes compared to that for the west target station to also accommodate ECR source. It included shield plug, service cap, containment box and ion source. Although diagnostic components were very similar in design, the fabrication and assembly took longer due to a manpower shortage in the Diagnostics group.

### Target Conditioning Box

An alternative conditioning system was designed and fabricated by December to expedite the process of changing and conditioning ISAC targets. Assembly was delayed to January, 2002, due to lack of manpower.

### HEBT

After completing HEBT1 (up to upstream of benders to DRAGON and TUDA beam line), and delivering beam to 1.5 MeV/u in December, 2000, resources were focused to complete chopper and bunch rotator (July), and 11 MHz buncher (September).

### Low Energy Experiments

These included moving GPS1 to a new location, modifications to LTNO and yield station, and  $\beta$ -NMR (new polarimeter, modifications to laser system, HV platform, and Oxford magnet). Extensive work was done on planning, coordinating and expediting activities and critical components from the Machine Shop

and outside suppliers for  $\beta$ -NMR, laser polarization systems, spectrometer, and associated LEBT components. The first data run on  $\beta$ -NMR was completed in the summer with polarization >65%, platform operation at 24 kV, and new polarimeter. Among other low energy experiments, the Osaka beam line was installed and tested in October/November with new chamber and associated services. The  $8\pi$  beam line with a simple chamber was installed and commissioned with a test beam in December.

### High Energy Experiments

These involved DRAGON and TUDA. Installation of HEBT components up to the TUDA experimental station, with associated services, was finished in March. A special room was designed and constructed for the TUDA detector system electronics, with all services and a special grounding system. The first stable beam to TUDA was delivered in March. First RIB was delivered to TOJA in June, and to TUDA in September, after commissioning the 11 MHz buncher.

### DRAGON

After completing installation of most components up to MD2 in December, 2000, the overall progress on DRAGON installation was relatively slow due to lack of technical resources. Several initial tests were done to commission the gas targets with its control system. Alpha tests up to the charge slits were done in January, and continued down the line as services were completed. DRAGON was commissioned with stable beam in October, followed by RIB in November.

### ISAC-II

PERTs were prepared that included work on specifications and design of a superconducting rf test facility and dummy cavity. A construction contract was awarded in October, and a test facility at B.C. Research was constructed at the end of November. Plastic roof and doors for the clean area, and hoist delivery was delayed to January, 2002. A Nb cavity was received from Legnaro in early summer. A dummy cavity was tested in a cryostat (without rf) in October, and (with rf) in December, with a plan to repeat these tests at B.C. Research in early February, 2002, followed by cold tests on the Nb cavity with rf controls in March, 2002. Milestones were established for the ACOT meeting in November, with an aim to be ready for 5.8 MeV/u at  $A < 60$  by April, 2005. Detailed schedules of ISAC-II projects were prepared that included: medium-beta cavities (with cryostats, refrigeration system and solenoid, with an aim to test first cryo module by summer, 2003); high-beta cavities system; charge state booster system which included tests on test stand with an aim to order CSB by December,

and test the whole system in the test stand by October, 2003; HEBT transfer system and H<sup>-</sup> HEBT to experimental stations.

### CONTRACT ADMINISTRATION

In the past year four contracts were awarded: Brandt Industries Ltd. of Saskatchewan manufactured the east target module and the east exit #1 and exit #2 modules. Brandt also manufactured the east dump and east entrance modules under a second contract.

Sunrise Engineering Ltd. of British Columbia manufactured the poles for the beam line 2A 15° switching dipole magnet. Sunrise also assembled the magnet, with Sigmaphi of France supplying the coils.

### Personnel Resources

In 2001 the average monthly personnel effort for ISAC decreased by approximately 7.6 people to an average of 76.15 FTE people per month (see Fig. 161). In 2000 the FTE effort per month was 83.75 people. The decrease was mainly due to a change in the monitoring system of personnel effort. Effective September 1, 2001, the recording of effort for the science facilities ended as the science construction phase was considered complete.

The average monthly personnel effort per system in 2001 (see Fig. 162) is described in Table XXXII.

Table XXXII. Personnel effort per system.

System	Monthly FTE
Project management & administration	3.90
Beam line 2A	1.35
Target station	9.33
LEBT	6.49
Accelerator	11.77
Science facilities (TRIUMF personnel)	13.40
Science facilities (non-TRIUMF personnel)	1.42
Infrastructure	8.91
Integration	16.89
ISAC-II	2.69
<b>Total average FTE monthly personnel</b>	<b>76.15</b>

Figure 163 shows the average monthly FTE personnel working on ISAC for the year 2001 based on the type of personnel.

The average monthly FTE personnel effort per system spent on ISAC science for the year 2001 is shown in Fig. 164. Note that the monitoring of personnel effort for ISAC science was discontinued August 31 as construction was considered complete.

The total personnel effort for ISAC since the start of the project January 1, 1996 to December 31, 2001 has been 422.77 years of work, based on a FTE work-month of 150 hours per person.

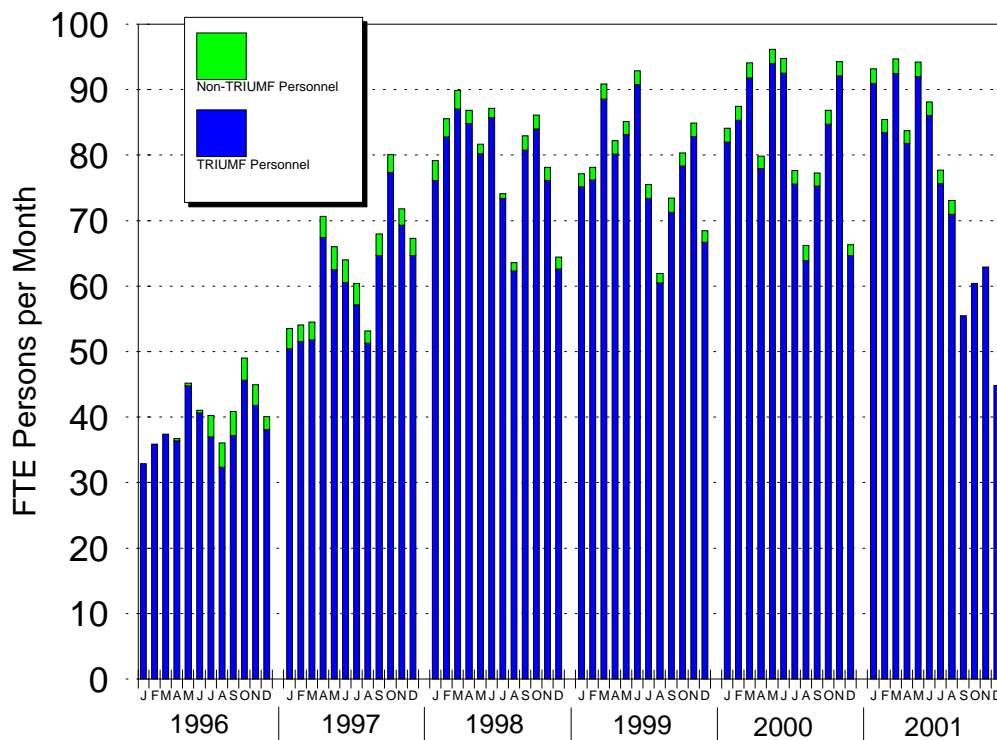


Fig. 161. ISAC monthly personnel effort, January 1, 1996 to December 31, 2001.

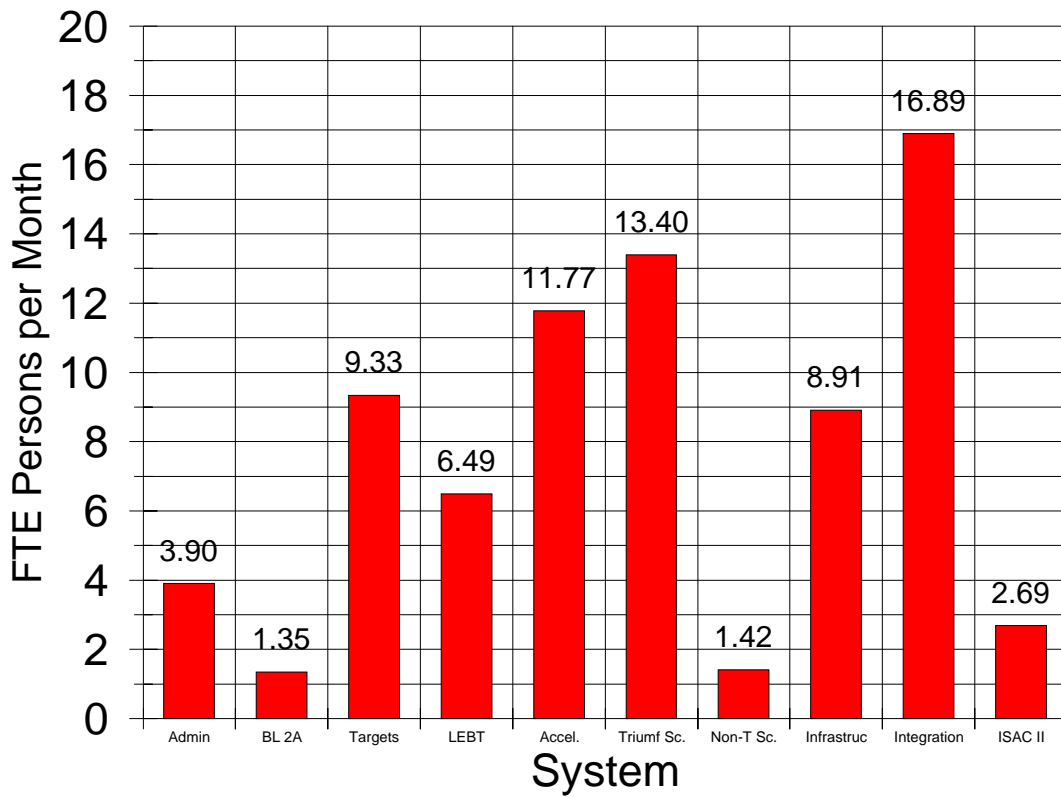


Fig. 162. ISAC average monthly personnel effort, shown by system for 2001.

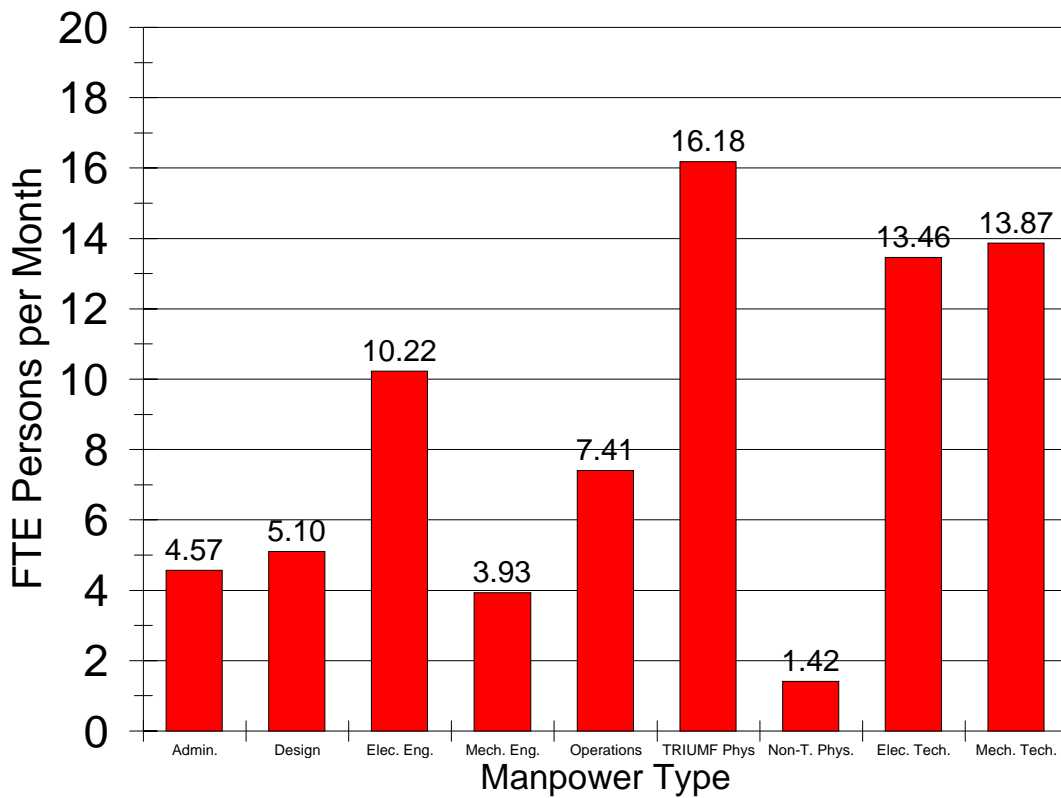


Fig. 163. ISAC average monthly personnel effort, shown by personnel type for 2001.

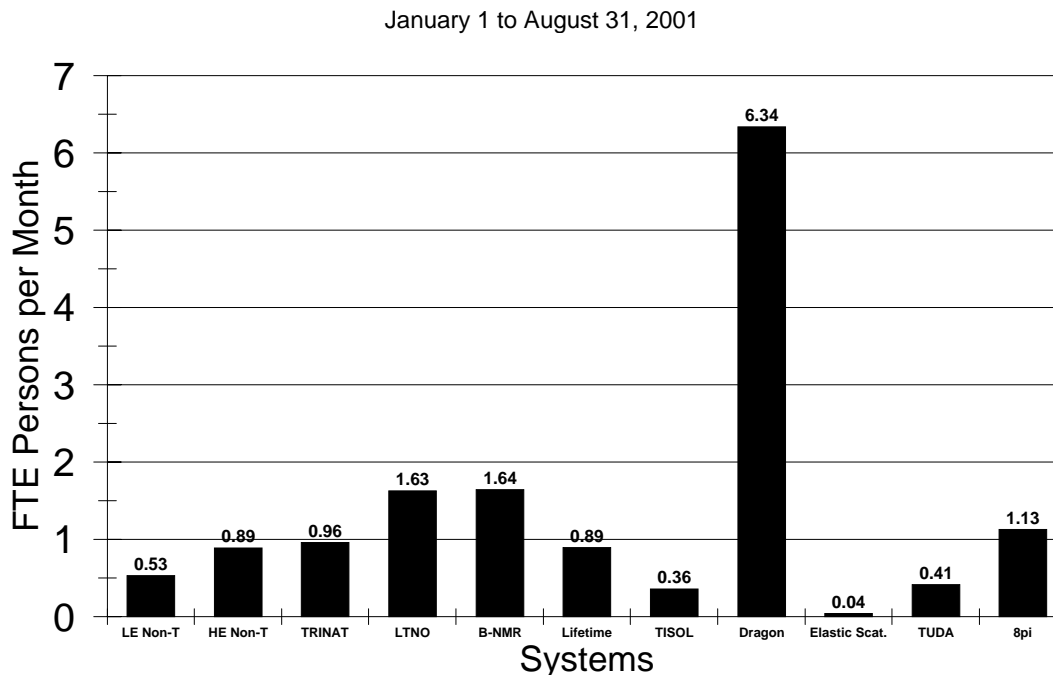


Fig. 164. ISAC average monthly personnel effort, science facilities, for January 1 to August 31, 2001.

## CONVENTIONAL FACILITIES AND INFRASTRUCTURES

ISAC continued to be the focus of the engineering and installation efforts. The ISAC-II expansion project received funding approval in April and was kick-started in earnest in May. Close coordination work continued with the Accelerator groups, the Engineering group and the Science Division for the installation and commissioning of the experimental facilities. This included attendance at regular and engineering meetings and participation in the engineering design review.

### Mechanical Services

ISAC consumed a majority of the 2001 effort. ISAC experimental hall completion comprised a wide range of work including cooling water, compressed air, and vacuum lines to HEBT and experimental areas, completion and commissioning of the DRAGON hydrogen exhaust system, gas tubing and alarms. Other ISAC completion jobs included a third controlled temperature water loop for TRINAT, mechanical penthouse hay loft hoist, connection and commissioning alarms for 6 fume hoods, spent target vault ventilation and exhaust, high level alarms for the three filling points for the decontamination sump, and vacuum roughing lines to the CDS room. One ISAC development job was the modification of experimental hall roof top heating units to act as exhaust fans for summer operation, and the installation of a test area of open floor grating on the mezzanine. This action is intended to reduce the air temperature on the mezzanine in summer, by moving

more outdoor air through the building, and allowing it free convection access to the mezzanine. Other development jobs included modification to chilled water supply lines to the electrical room to allow more efficient operation of chiller 2 in winter, venting the decontamination and sanitary sumps for odour control, and DDC operational improvements. A list of MRO work was carried out.

Engineering assistance was provided for the ISAC-II building project, and the SCRF room at B.C. Research.

### Electrical Services

Engineering efforts focused on the experimental facilities, the target conditioning facility and the east target. Completed tasks included services for experiments like DRAGON, TUDA,  $8\pi$ , the polarimeter, Osaka, and the power distribution for the 60 kV bias target conditioning system. The 60 kV bias distribution for the mass separator was also completed. For the MEBT a new supply and wiring were provided to accommodate a new Stinson steerer, which replaced an AECL steering magnet. About 40 installation orders were processed for ISAC alone. The largest single task was the design of the grounding and the ac power distribution for the east target ion source terminal. The initial target grounding concept was revised and expanded to include the east target. The experience gained with the operation of the west target ion source led to changes to the initial grounding scheme

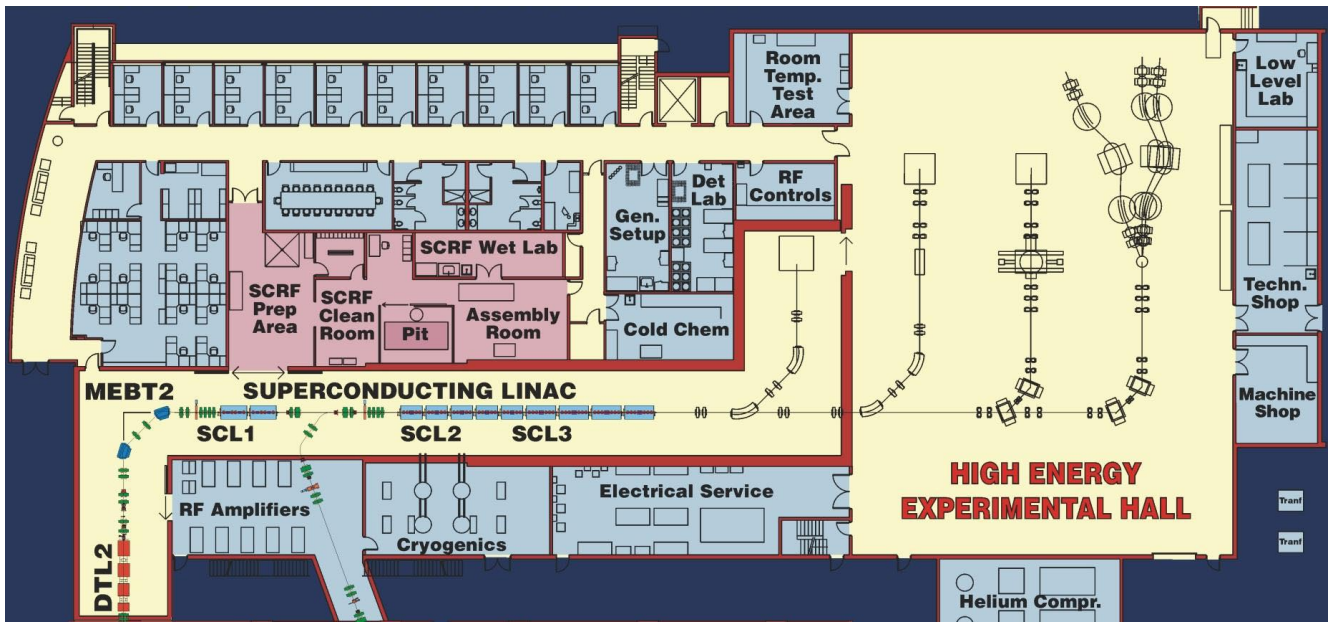


Fig. 165. ISAC-II expansion: ground floor.

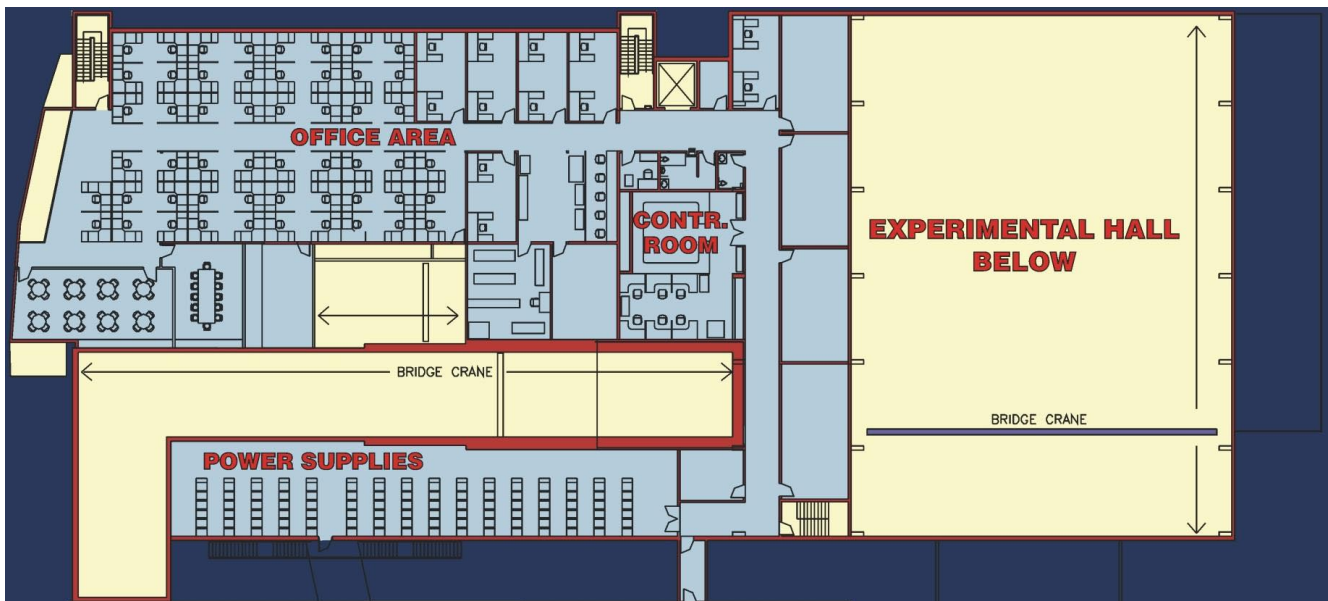


Fig. 166. ISAC-II expansion: upper floor.

proposed. The new concept is based on the idea of a “STAR” grounding referenced to the mass separator. This is used as the common signal reference ground point (SRG) for both target systems. Apart from this common point, the east target SRG is completely separated from the west target SRG. This evolution came about to eliminate problems associated with potential ground loops – and associated operational disruptions – between the two target systems. Installation of the services for the east target station is still in progress with commissioning scheduled for winter, 2002.

The conduit installation for the various radiation systems and the HV interlock systems was extensive.

On the maintenance front we had a couple of serious problems to address. The RFQ main contactor relay started malfunctioning during the fall. The over-current protection function was not working properly. It will be replaced during the winter shutdown. On December 15, a severe wind storm hit the Lower Mainland causing a series of successive power outages of the 60 kV transmission line to the UBC campus. One of the ISAC power distribution centres feeding the mechan-

ical services, MCC-X, suffered a partial short circuit and caught fire. The electrical crew had to work around the clock to restore service and minimize disruption to the experimental program.

### ISAC-II Conventional Construction

The buildings portion of the ISAC-II expansion project started in earnest upon receiving funding approval from the provincial government in April. The Province funded the base request of \$8.7 M through the B.C. Knowledge Development Fund, in support of the experimental program. \$1.0 M was added by TRI-UMF to build much needed office space for research and technical staff that has been housed in temporary trailers for a long while. UMA Management Services Ltd. was appointed as project manager in early June, followed shortly thereafter by the appointment of PBK Architects Ltd. and Cochrane Engineering Ltd. for the architectural and the engineering design.

The new expansion will be built to the north of ISAC-I. It includes office space for about 90 research and technical staff, laboratory and technical support space, the accelerator and support functions, building services and a high-energy experimental hall (see Figs. 165 and 166). The total finished floor space is approximately 55,000 sq ft. The construction site will be very busy throughout 2002 due to space limitations and the concurrent construction of the MDS Nordion TR30-2 project.

The project went through a very involved approval process with the University of British Columbia and the Province of British Columbia. The process included planning committees, advisory design committees, design review committees, public hearings and four board meetings. The development permit was issued in November.

The conceptual design was fully developed by the end of the summer. The detailed design was near completion by year-end.

Preparatory work, including the office trailer relocation and the relocation of the 69 kVA power line from the ISAC-II building footprint, was completed during the fall.

The construction was broken down into two main packages: the site preparation package to allow for the advancement of the work, and the main building package to take the building to completion. The site preparation package was tendered and awarded in December with construction scheduled for completion in February, 2002. The tendering of the main building package is slated for late January, 2002 with substantial completion scheduled for December, 2002 and beneficial occupancy in January, 2003.

### ISAC-II ACCELERATOR

In the past year the ISAC-II accelerator design and prototyping was advanced on a number of fronts:

- In an effort to finalize the building layout, realistic designs for transport lines and accelerators were developed and simulated. This set the position for the SC-DTL in the new hall at  $(x, y) = (15.66, 19.0)$  m with respect to the ISAC accelerator N-S, E-W intersection point as reference.
- An optimized cryomodule concept was developed to maintain a more consistent beam envelope throughout the linac.
- Multi-charge particle dynamics were simulated in the code LANA, complete with transfer lines, isopath bend sections and realistic cryomodule dimensions.
- A two stage installation scenario was advanced. In a first stage, the full energy 1.5 MeV/u beam from the ISAC DTL-I will be transported via the HEBT transfer line from the ISAC-I E-W beam line to the ISAC-II E-W beam line and injected into the medium- $\beta$  section of the ISAC-II superconducting linac. Up to seven cryomodules may be installed in the original installation with all five medium-beta modules (twenty cavities) and up to two high-beta modules (twelve cavities) giving  $E = 5.8$  MeV/u for  $A/q = 6$ . In the final stage, the low-beta cryomodule (eight cavities) and last high-beta cryomodule (eight cavities) would be added for  $E = 6.5$  MeV/u for  $A/q = 7$ . Beam transport was designed assuming that the future installation would be compatible with the existence of the initial installation.
- A medium- $\beta$  cavity prototype designed and built in collaboration with INFN-LNL was successfully tested in Legnaro. Specifications for the order of twenty medium- $\beta$  cavities were prepared.
- A SCRF test lab was established at B.C. Research and a test cryostat was designed, built and tested.

Figure 167 shows a schematic for the ISAC-II linac with stage 1 and stage 2 installations complete. The work is summarized below.

#### Linac Lattice

Beam dynamics simulations have been done to maintain the possibility of utilizing multi-charge acceleration in the ISAC-II superconducting linac to preserve beam intensity and/or allow the possibility of a second optional stripping stage to boost the final ion energy. In initial lattice studies, Legnaro/JAERI-style four cavity cryomodules were assumed, separated by



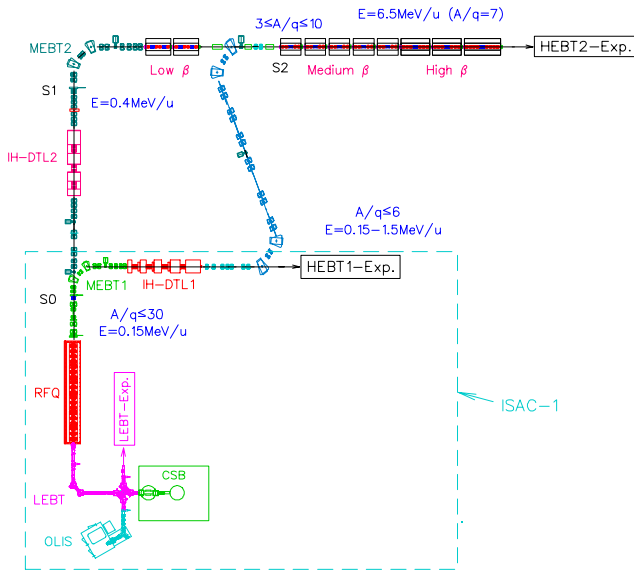


Fig. 167. A schematic for the ISAC-II linac with stage 1 and stage 2 installations complete.

focusing magnets at room temperature. The studies show that superconducting solenoids are the optimum focusing element for transporting beams with multiple-charge states.

The choice for superconducting solenoids allowed us to re-think the cryomodule specification with a goal to rationalize the transverse optics. Four different cryomodule layouts are now specified, one for each of the low- and medium-beta sections and two for the high-beta section (see Fig. 168). The number of focusing elements is varied along the accelerator length for a reduced transverse envelope and the diagnostic boxes are positioned at waists in the transverse envelopes. Beam dynamics studies in the low-beta cryomodule showed that we can reduce longitudinal emittance growth by using one long module of eight cavities and four solenoids. The last solenoid at the exit

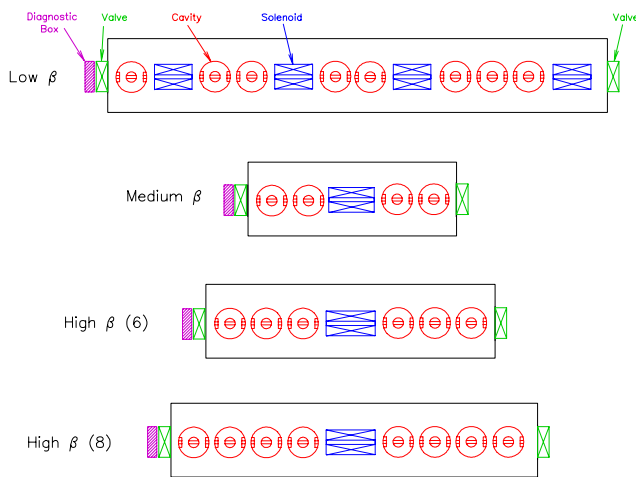


Fig. 168. Proposed cryomodule layout for the three sections of the ISAC-II SC linac.

of the cryomodule is used to help match the beam to the medium-beta section. The module has a length of 4.28 m from cell centre to cell centre. A cryomodule cell consists of the cavities, the solenoid(s), isolation valves and a diagnostics box. The cryomodule cell length for the four cavity medium-beta cryomodules is 2.09 m. In order to incorporate twenty high-beta cavities, it is considered to use two, six cavity cryomodules with a length of 2.76 m each and one, eight cavity cryomodule of 3.32 m. The new cryomodule concept also allows the possibility of optimizing the transverse dimensions of each cavity type. This will receive further study.

## Stage 1 Installation

### HEBT transfer

The HEBT transfer section transports the 1.5 MeV/u,  $B\rho \leq 1.22$  Tm beam from after DTL-I to the medium- $\beta$  section of the superconducting linac. The transfer section, shown in Fig. 169, is configured as an S-bend system composed of two symmetric doubly achromatic  $\sim 118^\circ$  bend systems with two, four quadrupole periodic transport sections joining the two bend sections. A 35 MHz buncher in between the two 4Q systems provides a longitudinal match to the medium- $\beta$  section of the SC linac. The second 4Q system matches the beam in the transverse planes to the medium- $\beta$  section of the SC linac.

Each achromatic bend is configured as a QQDQQDQQ system and transports the beam from double focus to double focus. The second achromatic bend has the extra condition of  $R_{12} = R_{34} = 0$  to allow transverse matching to the SCDTL by the upstream 4Q system. All dipoles are identical with rectangular poles.

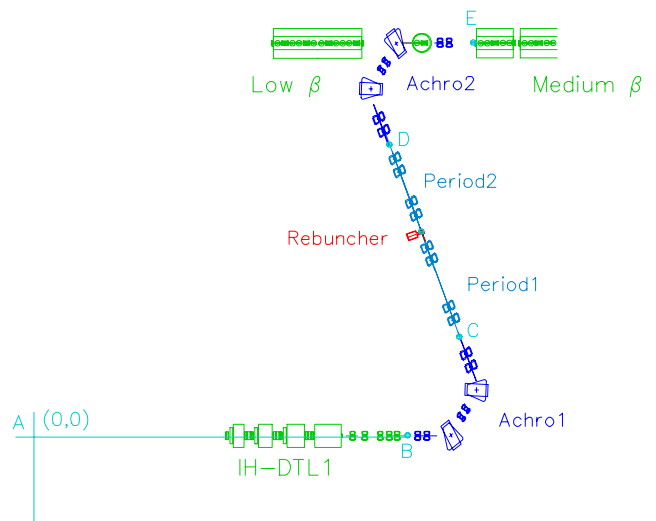


Fig. 169. The HEBT transfer line for ISAC-II stage 1.

## Linac optics for stage 1 installation

The transport and accelerator dynamics for stage 1 were simulated using LANA. The simulation includes all transport from the output of the ISAC DTL to the end of the 7-module ISAC-II SC linac. Thus far we have only considered cavity fields using a “square-wave” approximation. Realistic cavity fields will be added to the LANA model in the future. This means that no transverse components to the cavity fields have been added so far. Likewise no cavity or solenoid misalignments have been considered.

The complete transfer line plus the full seven cryomodules were simulated with LANA for two single charge cases corresponding to ions with  $A/q$  of 3 and 6. A summary of the the envelopes in the SC-DTL are shown in Fig. 170.

In both cases, matching and acceleration are straightforward. The lattice easily accommodates the rf defocusing from the high gradient cavities with only slight transverse emittance growth. Minor longitudinal emittance growth occurs due to the rather large debunching at the position of the 35 MHz rebuncher. We could also consider lowering the frequency of this buncher to avoid the growth.

Beam simulations were also done to study the multi-charge beam dynamics for the stage 1 installation. The reference ion for the multi-charge runs is  $^{132}\text{Sn}$  with an equilibrium charge state of  $Q_0 = 31$  when stripping at 1.5 MeV/u. For the simulations we assume a foil is inserted at the entrance of the medium-

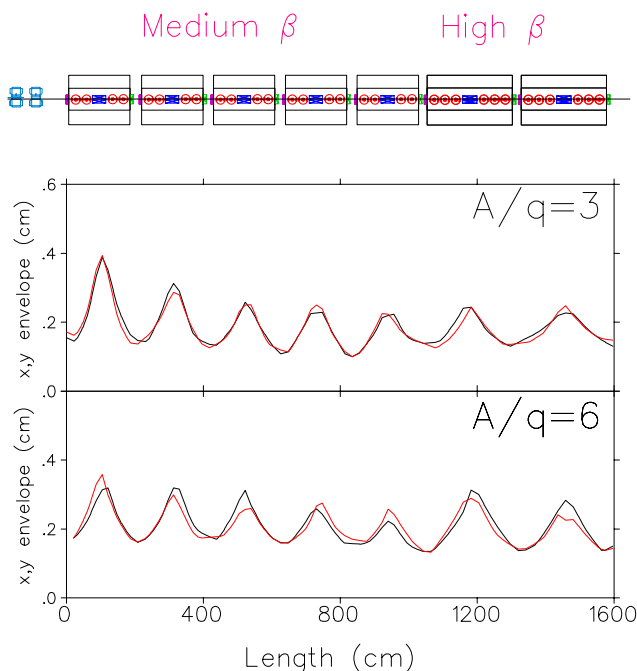


Fig. 170. Transverse beam envelopes are shown as a function of length for the SC-DTL (stage 1) for  $A/q$  of 3 and 6.

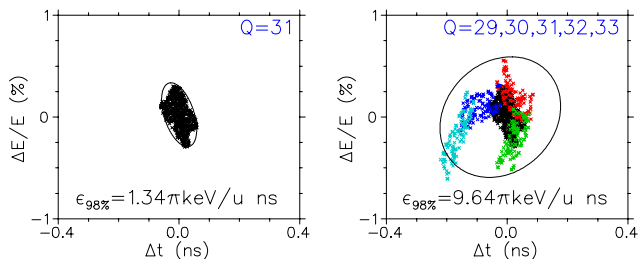


Fig. 171. Final longitudinal phase space ensembles for both a single charge state,  $^{132}\text{Sn}^{31+}$  (20% of the beam), and multiple charge states,  $^{132}\text{Sn}^{29+,30+,31+,32+,33+}$  (80% of the beam) after acceleration through the SC-DTL linac (stage 1).

beta section. Five charge states,  $Q = 29, \dots, 33$ , are accelerated through the SC linac. The transverse optics are very well behaved. The final phase ellipses are shown in Fig. 171. The longitudinal emittance is broadened since each charge ends up in a different region of phase space. The transverse emittance experiences relatively little increase.

## Stage 2 Installation

### Beam transport

The MEBT transfer section transports the beam from the ISAC-I MEBT to the IH-DTL-II in the N-S vault of the new ISAC-II building.

The beam is transported from the double focus at the MEBT-I stripping foil,  $(\beta_{x,y}) = 0.08 \text{ mm/mrad}$ , through two 4Q periodic transport cells to a double focus upstream of a matching section to the IH-DTL-II. A 35 MHz rebuncher at this double waist, plus a 4Q section, matches the beam to the new linac. The first section utilizes the first two quadrupoles of the charge selection section of MEBT-I with a central drift between doublets to accommodate the MEBT-I dipole. The optics from ISAC MEBT to IH-DTL-II are displayed in Fig. 172.

The second medium energy beam transport (MEBT-II) section is required to deliver the beam from IH-DTL-II to the low- $\beta$  section of the superconducting linac. As in the ISAC MEBT-I the transport is composed of three sections: a matching section to give a three dimensional focus on the stripping foil at 0.4 MeV/u, a 90° bend section for charge selection (or charge acceptance) and a matching section before the superconducting linac. The MEBT-II section is shown in Fig. 173. The design  $A/q$  is 30 before the stripping foil and 7 downstream of the stripping foil.

The first section is composed of six quadrupoles in a combination of two triplets to give a double waist near the centre of the section to allow the insertion of a buncher to give a time focus on the ISAC-II stripping foil.

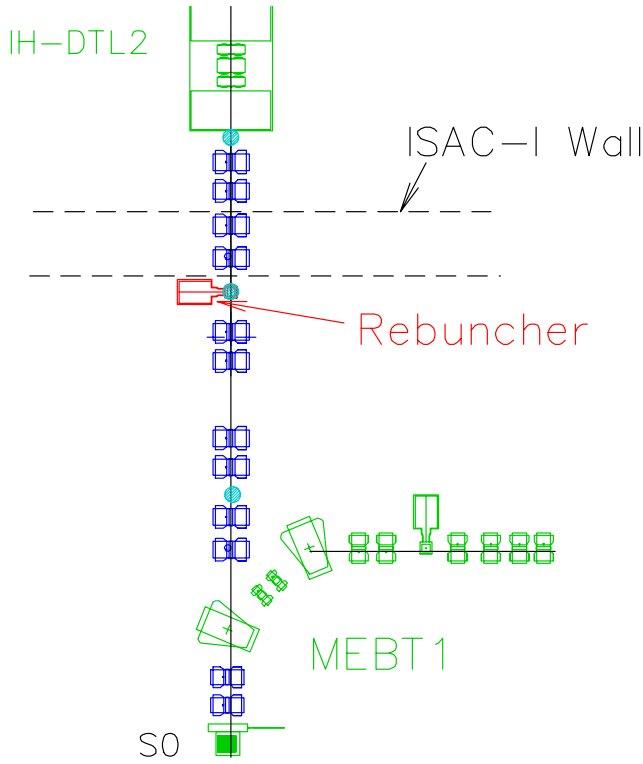


Fig. 172. The beam transport between ISAC MEBT and IH-DTL-II.

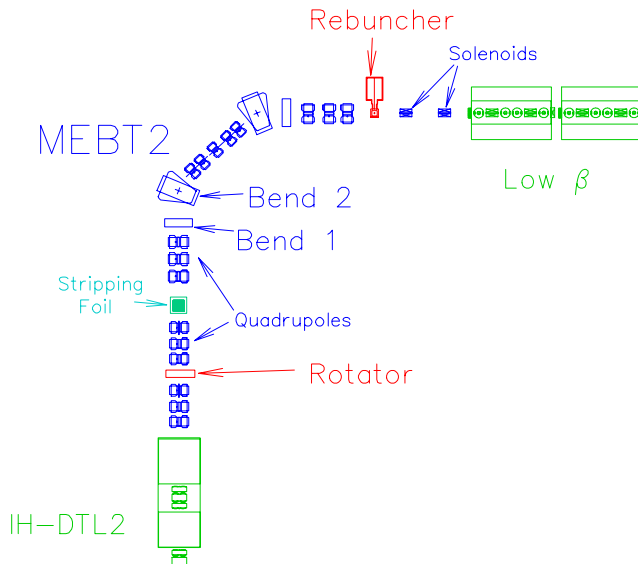


Fig. 173. The beam transport between IH-DTL-II and the low- $\beta$  section of the SC-DTL.

Since we want to maintain the possibility of multi-charge acceleration in ISAC-II, the charge selection section must be made not only achromatic but also isopath (same path length for each charge state) so that we maintain the proper phasing of the various charge states. A small reverse bend dipole is employed to provide a negative path difference dispersion that is cancelled by the path difference in the main dipole.

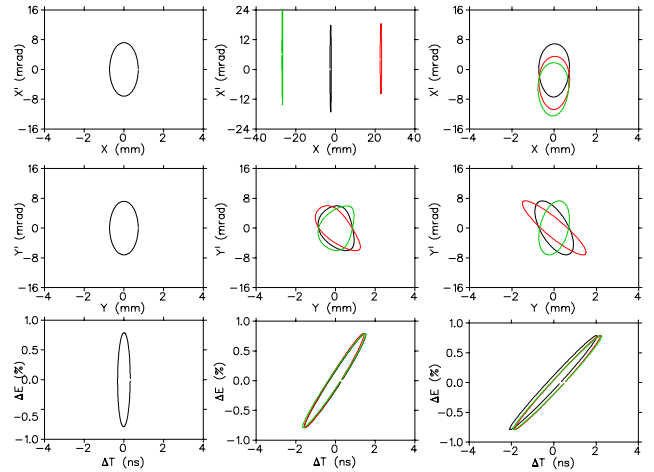


Fig. 174. Beam ellipses for horizontal (top), vertical (middle) and longitudinal (bottom) planes for three charge states,  $\Delta Q/Q = 0, +5\%, -5\%$  (black, red, green), at the stripping foil (left), mid-point (middle) and end (right) of the charge selection isopath section.

The quadrupoles between dipoles achieve the double achromaticity. Symmetric quadrupoles before and after the benders produce a unitary matrix in  $x$  and  $y$ . Higher order multipoles are added to provide correction due to the large perturbation caused by the relatively large differences in charge state,  $\Delta Q/Q = \pm 5\%$ . Beam simulation results showing beam emittances for three charge states,  $\Delta Q/Q = 0, +5\%, -5\%$ , are summarized in Fig. 174.

In order to provide a reasonable match for all ions with  $3 \leq A/q \leq 7$ , we chose a buncher position optimized for the lighter ions where the longitudinal acceptance is smaller due to the relatively strong accelerating gradient. A 35 MHz buncher is centred at the double focus provided by the isopath section. In order to optimize the acceptance of multi-charge beams, a system of two superconducting solenoids has been chosen over a four quadrupole system.

The beam transport section in between the low- $\beta$  and medium- $\beta$  sections of the SC-DTL will be installed to coexist with the HEBT transfer line components so that beams could be switched from one line to the other to allow flexibility in the operation.

The transport section in question takes the beam from the output of the low- $\beta$  accelerator with beam energy varying from 1.2 MeV/u to 2.3 MeV/u for ions ranging from  $A/q = 7$  to 3 respectively, and rebunches with a superconducting 70 MHz buncher followed by a solenoid to match the beam to the medium- $\beta$  section (Fig. 175).

### Linac simulations for stage 2

Beam simulations for the stage 2 installation include the complete beam transport from ISAC-II stripping foil, the low-beta SC-DTL section, the matching

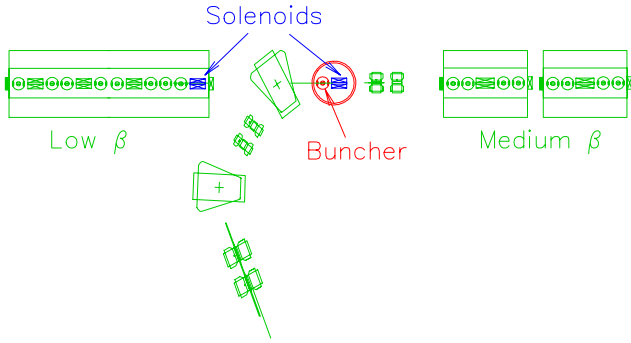


Fig. 175. The beam transport between the low- $\beta$  and medium- $\beta$  section of the SC-DTL.

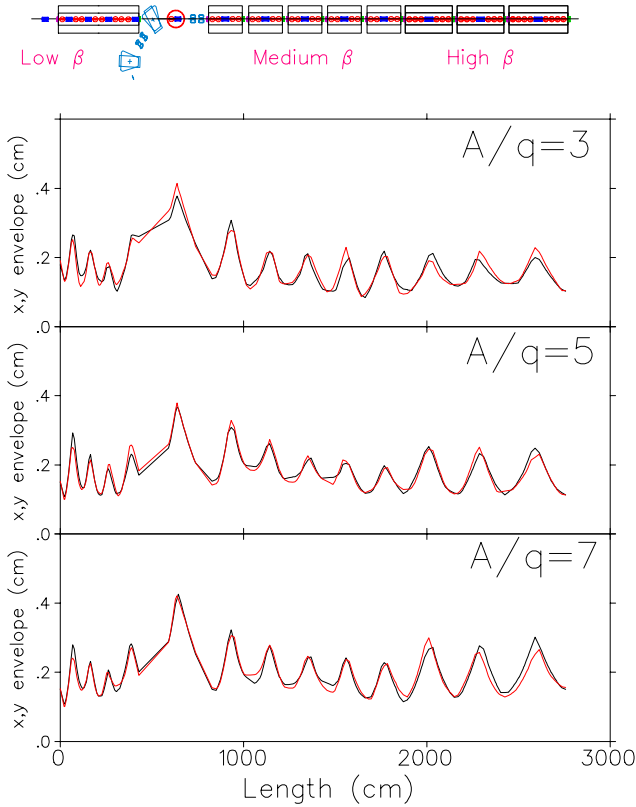


Fig. 176. Transverse beam envelopes are shown as a function of length for the SC-DTL (stage 2) for  $A/q$  of 3, 5 and 7.

between low- and medium-beta sections and the five medium and three high-beta cryomodules, for singly-charged ions with  $A/q = 3, 5, 7$ .

In all three cases, matching and acceleration deliver good quality beams. The ion dependent matching at the entrance to the low-beta section and between the low- and medium-beta sections does generate some small longitudinal emittance growth. A detailed plot of the beam envelopes for the acceleration only for the three cases is given in Fig. 176.

For multi-charge simulations, three possible stripping foil positions are considered: foil 1 at the ISAC-II

foil location before the isopath section, foil 2 at a position just upstream of the low-beta cryomodule and foil 3 at a position just upstream of the first medium-beta cryomodule. In the study, foil 1 and foil 2 positions are used interchangeably to show the effect of the imperfect isopath optics on the multi-charge beam dynamics. Foil 3 was added to simulate cases where the accelerator is configured in energy boost mode. In multi-charge runs, three charge states ( $^{132}\text{Sn}^{20+,21+,22+}$ ) are accelerated after foil 1 or foil 2, encompassing 57% of the beam, and five charge states ( $^{132}\text{Sn}^{30+,31+,32+,33+,34+}$ ) are accelerated after foil 3, encompassing 80% of the beam. By comparison, a single charge state ( $^{132}\text{Sn}^{21+}$ ) from foil 1 or foil 2 would encompass 21% of the beam, while a single charge state ( $^{132}\text{Sn}^{31+}$ ) from foil 3 would encompass 20%.

Simulations show that any combination of foil 2 and 3 produce beam envelopes with almost no discernable difference between the single-charge and multi-charge runs. This shows the inherent stability of the transverse lattice and inter-linac matching section. The final longitudinal phase ellipses comparing single-charge and multi-charge particle ensembles for different combinations of foil 2 and foil 3 cases for the stage 2 installation are shown in Fig. 177.

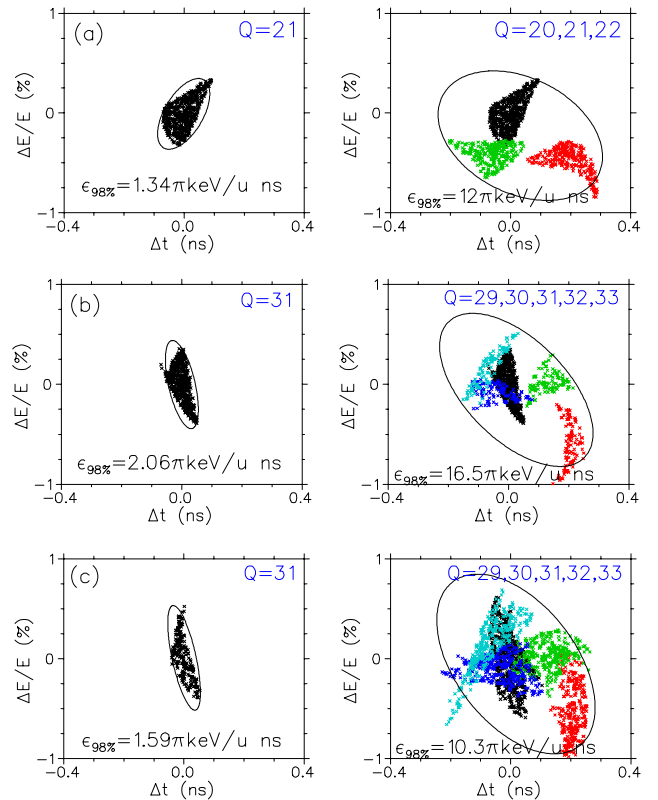


Fig. 177. Final longitudinal phase space ensembles for single- and multi-charge simulations of  $^{132}\text{Sn}$  for (a) foil 2 only (7.4 MeV/u), (b) foil 3 only (10.3 MeV/u) and (c) foil 2,3 (10.3 MeV/u) simultaneously.



In the case of foil 1 the three charges are somewhat mismatched, transversely, after the isopath section and have slightly different arrival times, leading to large envelope perturbations in the low-beta section. Some improvement is found by optimizing the accelerator to transport  $Q_0 = 20.4$  so that the accelerated charges will have relative errors of  $\Delta Q/Q = -2\%$ ,  $3\%$  and  $8\%$  from the linac tune. In this case the acceptance for the lowest charge is sufficient to contain the mismatched beam. One further problem is that at  $\Delta Q/Q = 8\%$  the transverse focusing strength of the linac lattice is near the stability limit and so transverse emittance growth, especially in light of the initial mismatch from the isopath, is increased. Nevertheless transmission is near 100% for the foil 1 multi-charge case.

### SCRF Developments

Although the program at TRIUMF is still in its infancy, a number of developments are under way including the fabrication and test of a medium-beta cavity prototype, the fabrication and cryogenic test of a test cryostat and the design of an SCRF laboratory.

#### Medium-beta cavity

A medium- $\beta$  quarter wave bulk niobium cavity has been designed in collaboration with INFN-Legnaro,

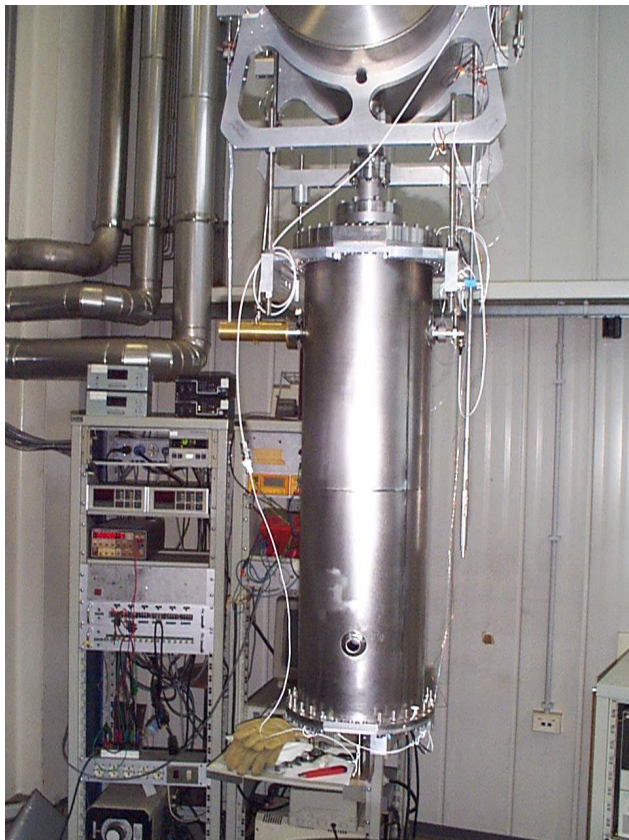


Fig. 178. TRIUMF medium-beta prototype cavity before cold test at INFN-LNL.

fabricated in Italy, received chemical polishing in CERN, and was rf tested in Legnaro. The cavity is shown in Fig. 178 prior to the first cold test. This cavity differs slightly from the Legnaro resonators in that the bottom tuning plate is now made from niobium sheet rather than sputtered niobium on a copper substrate, and additional rigidity has been added at the top plate to reduce the cavity detuning due to fluctuations in the pressure of the cryogenic system.

Multipactoring conditioning, started at room temperature, was completed during resonator pre-cooling with an elapsed time of about four hours. After cool-down to 4.2 K the cavity was pulse conditioned for 1 hour in  $3 \times 10^{-5}$  mbar helium. Results of the first rf test are shown in Fig. 179. The cavity performance exceeds the ISAC-II requirements with an accelerating gradient of 6.7 MV/m for 7 W dissipated at 4 K. A peak gradient of 11 MV/m was achieved. The cavity is now being prepared for further rf tests at TRIUMF.

Specifications for cavity fabrication are now being written. An order for twenty medium-beta cavities will be placed in industry early in the new year.

#### Test cryostat

A test cryostat has been designed and built in a collaboration between TRIUMF and Quantum Technologies of Whistler, B.C. The cryostat is shown in Fig. 180.

The cryostat vacuum vessel is 2.4 m high by 0.8 m in diameter. A LN<sub>2</sub> side shield holds a volume of 200 l and is directly connected to a copper bottom shield, baffled to allow adequate conductance for pumping. A top shield of copper is bolted to a copper flange at the top of the LN<sub>2</sub> vessel with bolt access available through six KF-50 flanges on the top plate. This copper flange is cooled by a copper cylinder inserted in the LN<sub>2</sub> vessel to a depth of 65 cm. The top plate assembly consists of two large flanges that allow separate removal of either the helium dewar/cavity assembly or the LN<sub>2</sub> vessel. The LHe vessel holds a volume of 48 l.

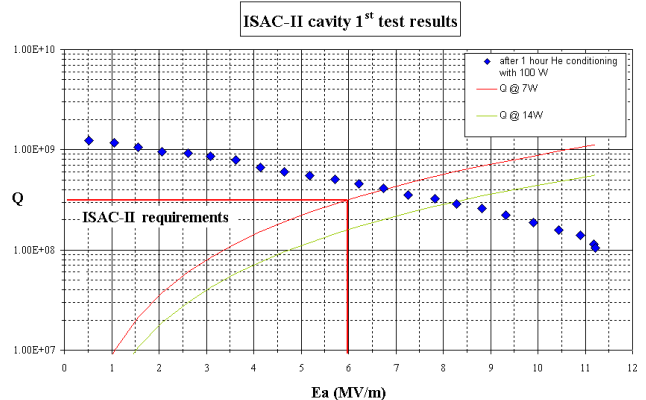


Fig. 179. Results of the first rf test on the medium-beta cavity at INFN-LNL.

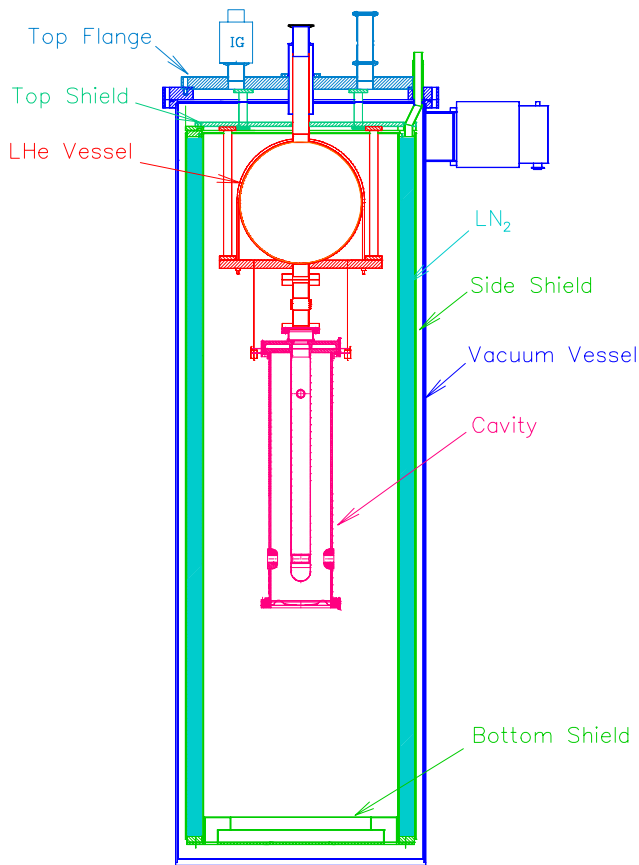


Fig. 180. ISAC-II test cryostat with cavity.

A “dummy”, full scale, medium-beta cavity has been fabricated in copper for cryostat tests and to establish test procedures. Initial cryostat tests have been completed. The top plate, top shield, LHe reservoir and dummy cavity are shown in Fig. 181 prior to assembly in the cryostat. The LHe boil off rate has been established by both measuring the flow of the escaping gas and by charting cavity temperature with time after a fill. A static heat load of 1.2 W was found corresponding to a boil off of 1.4 l/hr. The loss rate for LN<sub>2</sub> is 1.5 l/hr. The vacuum pressure in the cryostat was  $5 \times 10^{-7}$  while warm, and  $8 \times 10^{-10}$  torr while cold.

### SCRF test laboratory

A temporary superconducting rf test lab is now being installed in a space rented by TRIUMF at B.C. Research. It is intended that the space will be occupied for at least two years until the SCRF area in the new ISAC-II building is available for occupancy. We expect completion of the temporary lab space in two months. The laboratory includes a test area with a sunken cryostat pit for high field rf testing, and clean areas for cavity assembling and high pressure water rinsing (Fig. 182). The total space comes to  $\sim 100$  m<sup>2</sup>.



Fig. 181. ISAC-II test cryostat inner assembly with dummy copper cavity.

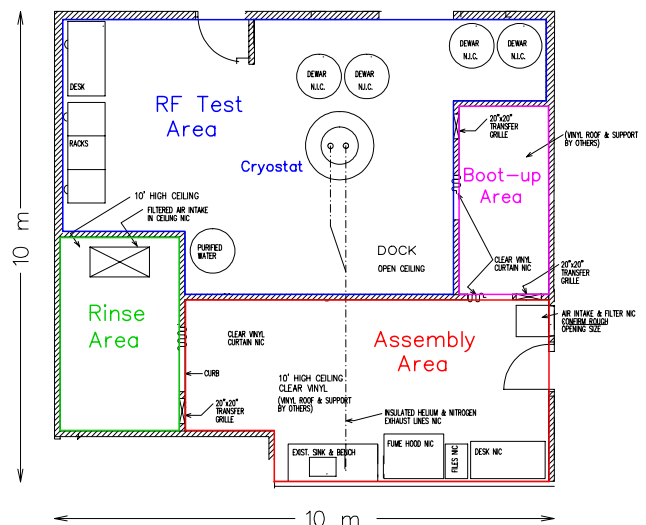


Fig. 182. The SCRF test facility being installed at B.C. Research.